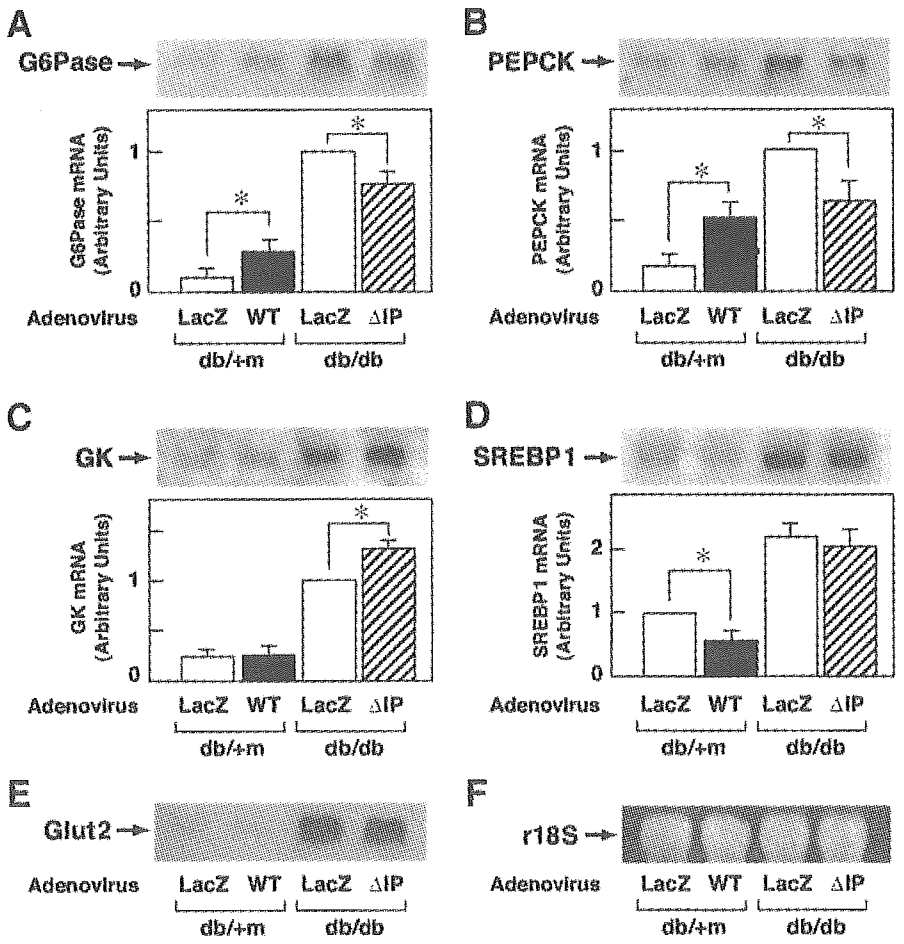

FIG. 4. Effect of SHIP2 expression on hepatic gene expression in db/+m mice and *db/db* mice. Total RNA isolated from the liver of WT-SHIP2– or LacZ-injected db/+m mice and ΔIP-SHIP2– or LacZ-injected *db/db* mice was subjected to Northern blotting with probes for G6Pase (*A*), PEPCK (*B*), GK (*C*), SREBP1 (*D*), and Glut2 (*E*) mRNAs and r18S (*F*). Results are representative of four separate experiments and shown as means ± SE *$P < 0.05$ vs. the level of expression in LacZ-transfected mice.

mice and in that of ΔIP-SHIP2– and LacZ-expressing *db/db* mice (Fig. 6).

Blood glucose and plasma insulin concentrations during oral glucose tolerance and insulin tolerance tests in SHIP2-expressing db/+m and *db/db* mice. Because the liver-specific expression of SHIP2 affected hepatic insulin signaling leading to the altered expression of genes implicated in glucose homeostasis, we examined the effect of liver-specific SHIP2 expression on glucose and insulin tolerance in db/+m and *db/db* mice. The blood glucose concentration at 30 min after oral glucose intake was higher in WT-SHIP2–expressing db/+m mice than LacZ-expressing db/+m mice (Fig. 7*A*). Plasma insulin concentrations remained higher at 0, 15, and 30 min after the glucose loading in WT-SHIP2–expressing db/+m mice than in LacZ-expressing db/+m mice (Fig. 7*B*). The kinetics of blood glucose concentrations after the insulin injection was comparable between WT-SHIP2– and LacZ-expressing db/+m mice (Fig. 8*A*). On the other hand, the basal glucose concentration was significantly reduced and the plasma insulin concentration tended to be decreased in ΔIP-SHIP2–expressing *db/db* mice compared with LacZ-expressing *db/db* mice. In addition, blood glucose levels (Fig. 7*C*) and plasma insulin concentrations (Fig. 7*D*) were significantly lower in ΔIP-SHIP2–expressing *db/db* mice than in LacZ-injected *db/db* mice at 15, 30, and 60 min after oral glucose intake. Furthermore, blood glucose levels were lower in ΔIP-SHIP2–expressing *db/db* mice than in LacZ-expressing *db/db* mice before and after the insulin injection (Fig. 8*B*).

DISCUSSION

A previous study (13) with knockout mice demonstrated that SHIP2 plays an important role in the negative regulation of the metabolic action of insulin in vivo. SHIP2 also appears to be implicated in type 2 diabetes with insulin resistance (14,15). Although the functional impact of SHIP2 on insulin signaling has been studied in cultured fat and skeletal muscle cells in vitro (16–22), the impact in vivo of hepatic SHIP2 on glucose metabolism in nondiabetic and diabetic states is unknown. Thus, it would be interesting to clarify how a hepatic excess of SHIP2 promotes insulin resistance and how the inhibition of hepatic SHIP2 ameliorates glucose metabolism in a state of insulin resistance in mice. We have shown that the systemic infusion of adenoviral vectors encoding WT-SHIP2 and a dominant-negative mutant of SHIP2 (ΔIP-SHIP2) in mice resulted in liver-specific expression of the protein.

We utilized db/+m mice as an animal of lean nondiabetic control. The liver-specific overexpression of WT-SHIP2 impaired insulin-induced phosphorylation of Akt without affecting tyrosine phosphorylation of IRS-1 and IRS-2 in the liver. Approximately a 50% decrease in the phosphorylation of Akt was observed even after the overexpression of WT-SHIP2 to a level more than fivefold that of endogenous SHIP2, as shown in Fig. 2*C*. As a cause of partial inhibition of the phosphorylation, we assume that SHIP2 product PI(3,4)P2 has some signaling ability to transmit the signal for the phosphorylation of Akt, al-

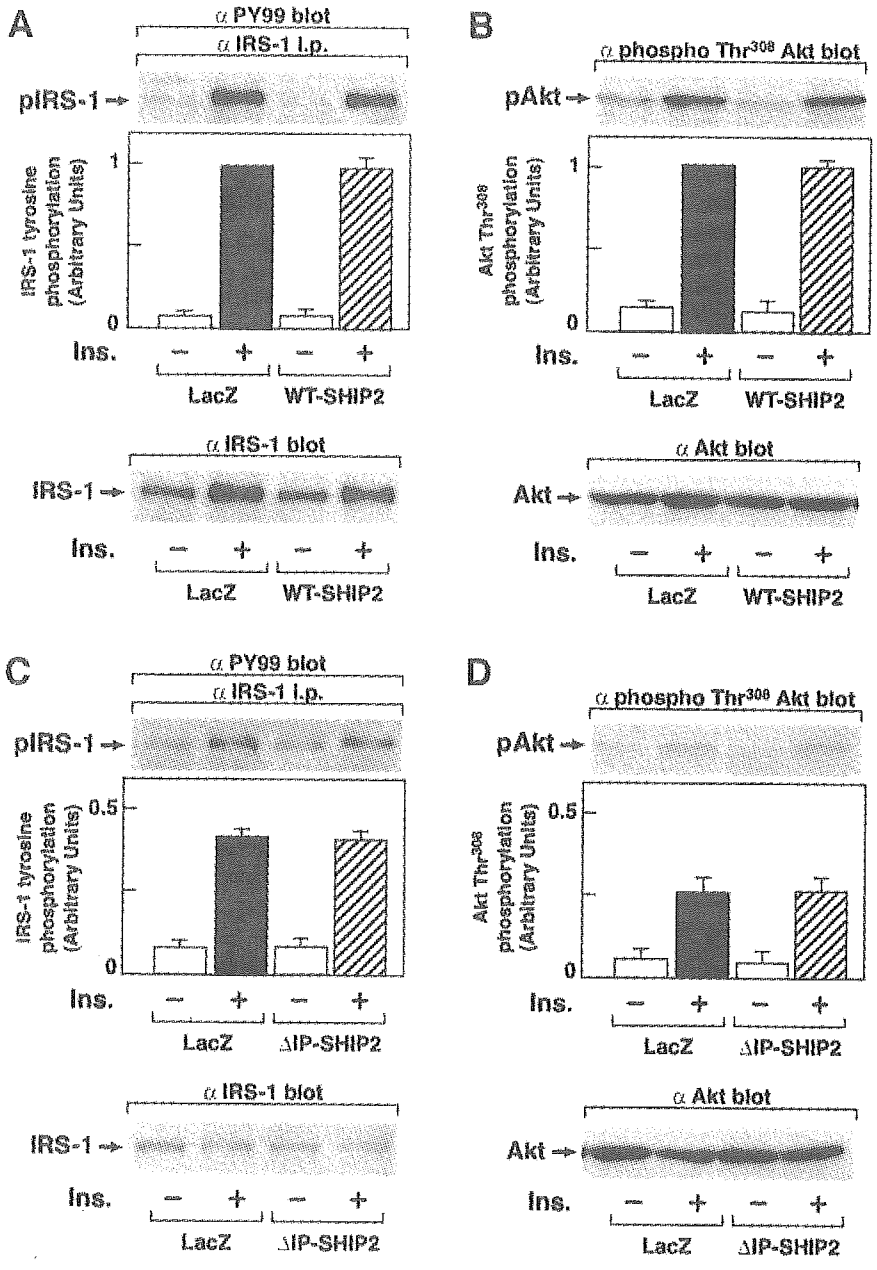

FIG. 5. Expression of SHIP2 did not alter insulin (Ins.)-induced phosphorylation of IRS and Akt in the skeletal muscle of db/+m and *db/db* mice. WT-SHIP2– or LacZ-injected db/+m mice (*A* and *B*), and ΔIP-SHIP2– or LacZ-injected *db/db* mice (*C* and *D*) starved for 16 h were injected with insulin (5 units/kg) via the tail vein. After 5 min, the skeletal muscle of the mice was excised and homogenized. Tissue samples were immunoprecipitated with anti–IRS-1 antibody. The precipitates were subjected to immunoblot analysis with anti–IRS-1 antibody or anti-phosphotyrosine antibody (*A* and *C*). The tissue samples were immunoblotted with anti-Akt antibody or anti–phospho-Thr^{308}–specific Akt antibody (*B* and *D*). Results are means ± SE of four separate experiments. *$P < 0.05$ vs. the amount of Akt phosphorylated in LacZ-transfected mice. i.p., intraperitoneal.

though less ability than PI(3,4,5)P3 (18,19). The overexpression of SHIP2 also resulted in hyperinsulinemia and potentiated the increase in blood glucose levels after oral glucose intake. These results indicate that the excess of SHIP2 in the liver can cause systemic insulin resistance through inhibition of hepatic Akt activation in vivo. Our results are consistent with a previous study (35) showing the effect of the liver-specific expression of a dominant-negative mutant of PI 3-kinase (Δp85), indicating that the hepatic PI 3-kinase pathway plays an essential role in the metabolic action of insulin. Thus, either inactivation of PI 3-kinase or potentiated hydrolysis of the PI 3-kinase product in the liver appears to result in an exacerbation of glucose metabolism in vivo.

We next studied *db/db* mice as an animal model of type 2 diabetes with insulin resistance. Db/db mice are obese and show hyperglycemia and hyperinsulinemia (39,40). The amount of protein and the extent of insulin-induced phosphorylation of IRS-1 and IRS-2 were mildly and markedly reduced, respectively, in the liver of *db/db* mice compared with that of db/+m mice. In addition, insulin-induced phosphorylation of Akt was markedly suppressed in the liver of *db/db* mice. Interestingly, the liver-specific expression of ΔIP-SHIP2 effectively restored the decreased phosphorylation of Akt without affecting the tyrosine phosphorylation of IRS-1 and IRS-2 in the liver. The hepatic expression of ΔIP-SHIP2 reduced fasting blood glucose concentrations and improved elevated glucose levels and insulin concentrations after oral glucose intake in *db/db* mice. Consistent with a recently published article (41) showing that an absence of SHIP2 confers resistance to diet-induced obesity and hyperglycemia in mice, our results indicate that the inhibition of endogenous SHIP2 in the liver can effectively ameliorate hyperglycemia and hyperinsulinemia through an improvement of the Akt pathway in diabetic *db/db* mice. In addition, these results

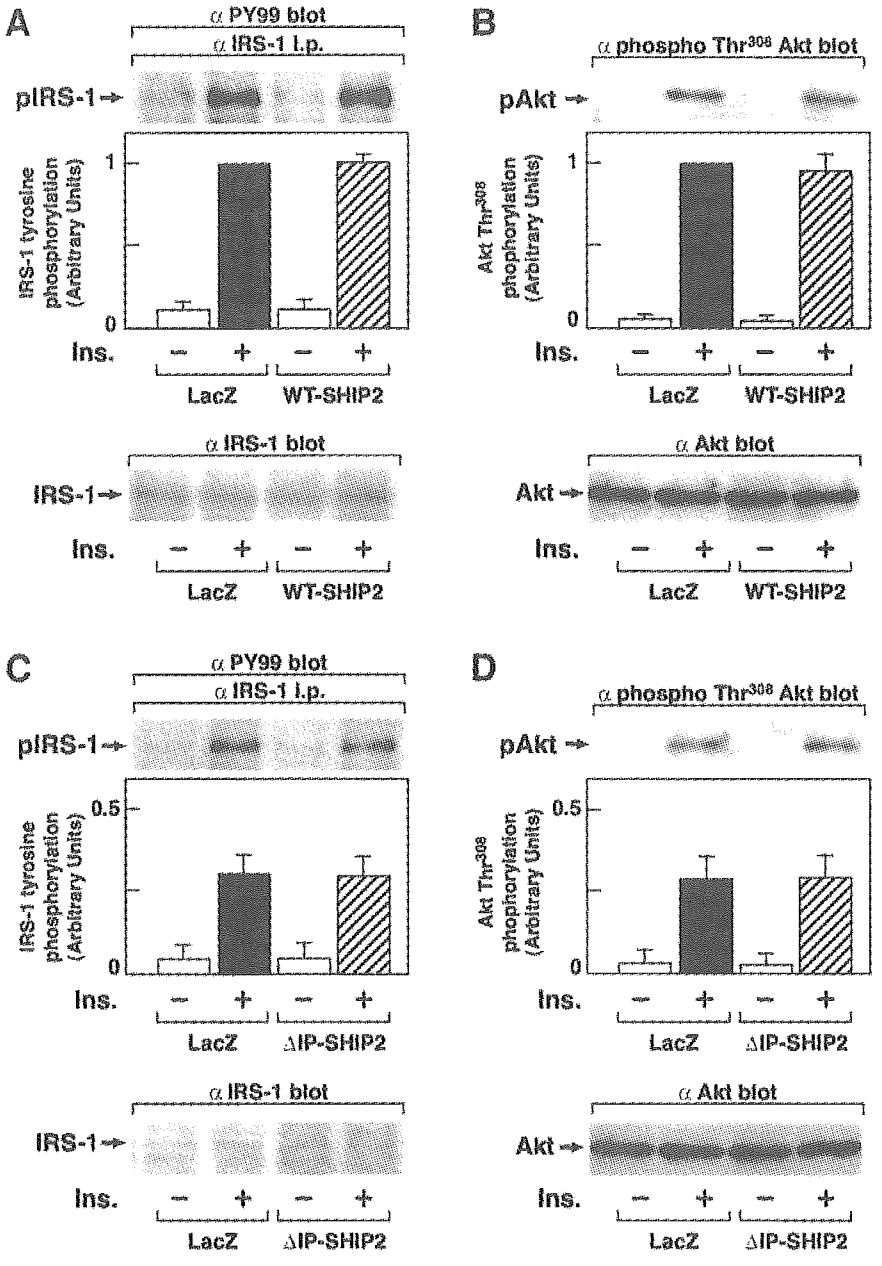

FIG. 6. Expression of SHIP2 did not alter insulin (Ins.)-induced phosphorylation of IRS and Akt in the fat tissue of db/+m and *db/db* mice. WT-SHIP2– or LacZ-injected db/+m mice (*A* and *B*), and ΔIP-SHIP2– or LacZ-injected *db/db* mice (*C* and *D*) starved for 16 h were injected with insulin (5 units/kg) via the tail vein. After 5 min, the epididymal fat of the mice was excised and homogenized. Tissue samples were immunoprecipitated with anti–IRS-1 antibody. The precipitates were subjected to immunoblot analysis with anti–IRS-1 antibody or anti-phosphotyrosine antibody (*A* and *C*). The tissue samples were immunoblotted with anti-Akt antibody or anti–phospho-Thr^{308}-specific Akt antibody (*B* and *D*). Results are means ± SE of four separate experiments. *$P < 0.05$ versus the amount of Akt phosphorylated in LacZ-transfected mice.

are consistent with reports on the 3′-lipid phosphatase PTEN. The PI 3-kinase product PI(3,4,5)P3 can also be hydrolyzed by PTEN (42). Thus, inhibition of PTEN was found to enhance insulin signaling in the liver in studies using tissue-specific deletion and antisense approaches (43,44).

Tissue-specific knockout of the insulin receptor revealed the liver to be the most crucial organ in terms of glucose metabolism in vivo (23,24). Insulin regulates glucose metabolism in the liver by regulating hepatic gene expression (23,24). The conversion of glucose to glucose 6-phosphate catalyzed by GK is the initial step in the utilization of glucose (45). Conversely, the reaction catalyzed by G6Pase is the final step of in the production of glucose, and PEPCK is a rate-controlling enzyme of gluconeogenesis in the liver (29). In addition, the production of triglycerides is mediated by lipogenic enzymes mainly regulated in a SREBP1c-dependent manner in the liver, and the enhanced expression of SREBP1c is associated with insulin resistance by causing fatty liver (46). Insulin is known to rapidly inhibit hepatic gluconeogenic gene expression and suppress hepatic glucose output via an IRS-2–mediated PI 3-kinase–dependent pathway mainly involved in Akt signaling (25–28). On the other hand, insulin increases the expression of GK mRNA and SREBP1c mRNA via the IRS-1–PI 3-kinase pathway (30). Based on these findings, inappropriate increases in the mRNA expression of G6Pase, PEPCK, and SREBP1c and/or a reduction in the mRNA expression of GK can lead to systemic insulin resistance (29,45–48). Along these lines, transgenic mice with hepatic overexpression of G6Pase or PEPCK exhibited enhanced hepatic glucose output leading to hyperinsulinemia and hyperglycemia (49,50).

Our results show that the hepatic expression of G6Pase and PEPCK mRNAs was increased by the hepatic overex-

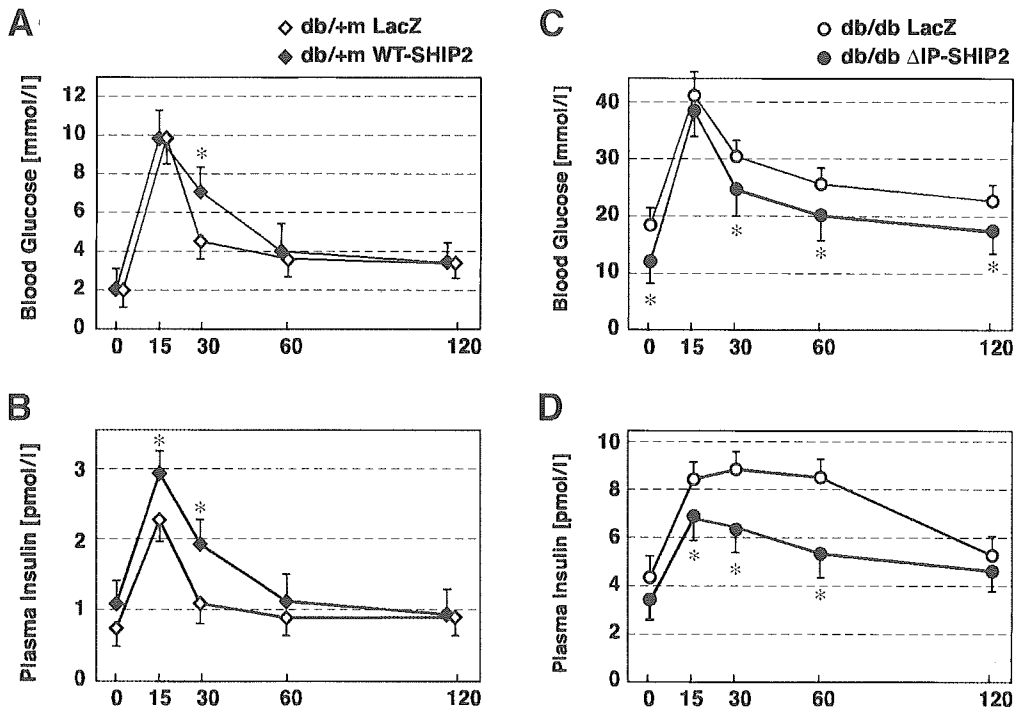

FIG. 7. Blood glucose and plasma insulin concentrations during oral glucose tolerance tests in SHIP2-expressed mice. WT-SHIP2– and LacZ-injected db/+m mice (*A* and *B*) and ΔIP-SHIP2– and LacZ-injected *db/db* mice (*C* and *D*) were starved for 16 h and then loaded orally with glucose (2 g/kg). Blood glucose levels (*A* and *C*) and plasma insulin concentrations (*B* and *D*) were measured at the indicated times after glucose loading. Results are means ± SE of four separate experiments. **P* < 0.05 vs. the corresponding value in LacZ-transfected mice.

pression of SHIP2 in db/+m mice. The apparent increase in blood glucose levels after the oral intake of glucose in the WT-SHIP2–expressing db/+m mice may be due to an impaired regulation of gluconeogenic gene expression leading to a reduced ability of the liver to dispose of glucose. The abundance of SREBP1 mRNA was reduced and that of GK mRNA was unaltered in the liver of WT-SHIP2–expressing db/+m mice. Based on the data, although the hepatic overexpression of WT-SHIP2 appears to regulate lipid synthesis through SREBP1c, the effect may have less of an impact on glucose metabolism than that caused by the altered levels of G6Pase and PEPCK mRNAs in the liver. On the other hand, the abundance of G6Pase, PEPCK, GK, and SREBP1c mRNAs was significantly increased in the liver of diabetic *db/db* mice. The inappropriately enhanced expression of G6Pase and PEPCK mRNAs was partially ameliorated, that of SREBP1 mRNA was unaltered, and that of GK mRNA was further increased in the liver of ΔIP-SHIP2–expressing *db/db* mice. Because these alterations of G6Pase, PEPCK, and GK mRNA expression are able to improve hepatic glucose disposal, the effect of hepatic ΔIP-SHIP2 expression on the improvement of hyperglycemia and hyperinsulinemia is considered to be mainly attributable to these changes in *db/db* mice. Notably, since hepatic glucose production is controlled by the expression of G6Pase and PEPCK in the liver, the improvement of glucose metabolism appears to be mainly caused by the inhibition of hepatic SHIP2 function leading to the appropriate regulation of hepatic glucose production. Fatty liver is possibly a result of the enhanced expression of SREBP1c mRNA in *db/db* mice. Since SREBP1 mRNA is already highly expressed in *db/db* mice, the enhanced PI 3-kinase–dependent signaling caused by the expression of ΔIP-SHIP2 may not have the effect of altering the expression of SREBP1 mRNA. Consistent with this interpretation, the extent of fatty liver was apparently unchanged by the expression of hepatic ΔIP-SHIP2 in *db/db* mice based on the histological analysis (data not shown).

After the oral intake of glucose, blood glucose levels and

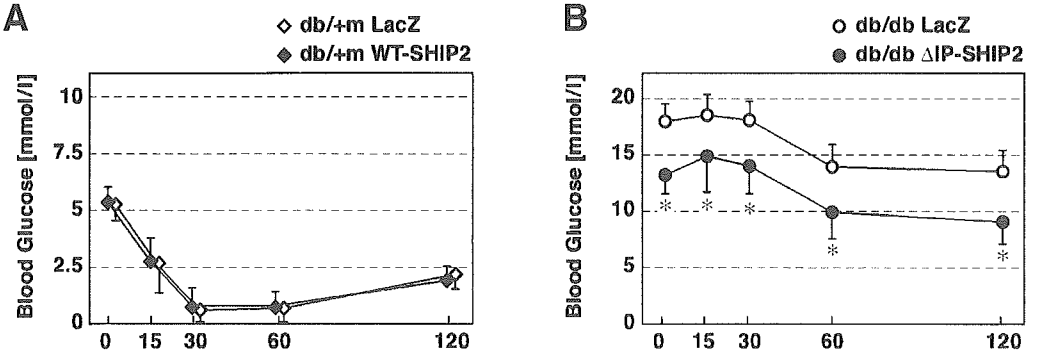

FIG. 8. Blood glucose levels during insulin tolerance tests in SHIP2-expressed mice. WT-SHIP2– and LacZ-injected db/+m mice (*A*) and ΔIP-SHIP2– and LacZ-injected *db/db* mice (*B*) were starved for 8 h and then injected intraperitoneally with insulin (0.75 units/kg). Blood glucose levels were measured at the indicated times after insulin injection. Results are means ± SE of four separate experiments. **P* < 0.05 vs. the corresponding value in LacZ-transfected mice.

serum insulin concentrations were elevated by the liver-specific expression of WT-SHIP2 in db/+m mice, but the increases were ameliorated by the liver-specific expression of ΔIP-SHIP2 in *db/db* mice. In contrast, blood glucose levels after intraperitoneal insulin injection were comparable between control LacZ- and WT-SHIP2–expressing db/+m mice. Fasting blood glucose levels were decreased by the hepatic expression of ΔIP-SHIP2 in *db/db* mice. The degree of the decrease in blood glucose levels appeared similar between LacZ- and ΔIP-SHIP2–expressing *db/db* mice at all time points after the intraperitoneal insulin injection. Because glucose levels after the intraperitoneal injection of insulin are mainly attributable to the effect of insulin on skeletal muscle and fat tissue (35), our results indicate that the effect of liver-specific expression of SHIP2 may be limited to the hepatic actions of insulin without affecting actions in the skeletal muscle and fat tissue. In this regard, insulin-induced tyrosine phosphorylation of IRS-1 and IRS-2 and phosphorylation of Akt at Thr^{308} and Ser^{473} were not affected in the skeletal muscle and fat tissue by the liver-specific expression of either WT-SHIP2 in db/+m mice or ΔIP-SHIP2 in *db/db* mice (Figs. 5 and 6 and data not shown). Our results partly contrast with a previous report (35) on the effect of liver-specific expression of Δp85. Inhibition of hepatic PI 3-kinase for 3 days affected insulin signaling in fat tissue, but not in skeletal muscle, to some extent (35). These possible differences may arise from the relatively minor alterations of blood glucose levels and insulin concentrations caused by the expression of WT-SHIP2 compared with those caused by the expression of Δp85. In this context, we cannot rule out the possibility that the skeletal muscle and/or fat tissue are involved, at least in part, in the alteration of glucose homeostasis caused by the liver-specific expression of SHIP2 in mice. More studies will be necessary to clarify this issue.

In summary, our results indicate that *1*) the liver-specific expression of SHIP2 regulates insulin-induced phosphorylation of Akt in the liver, but not in the skeletal muscle and fat tissue, *2*) elevation of SHIP2 expression in the liver has an impact on the deterioration of glucose metabolism in vivo, and *3*) the inhibition of SHIP2 function in the liver is an effective approach for the amelioration of hyperglycemia with insulin resistance.

ACKNOWLEDGMENTS

This work was supported in part by a Grant-in-Aid for Scientific Research from the Japan Society for the Promotion of Science and by a grant for research on sensory and communicative disorders by the Ministry of Health, Labor, and Welfare, Japan.

REFERENCES

1. Khan AH, Pessin JE: Insulin regulation of glucose uptake: a complex interplay of intracellular signalling pathways. *Diabetologia* 45:1475–1483, 2002
2. Saltiel AR, Kahn CR: Insulin signalling and the regulation of glucose and lipid metabolism. *Nature* 414:799–806, 2001
3. White MF: IRS proteins and the common path to diabetes. *Am J Physiol Endocrinol Metab* 283:E413–E422, 2002
4. Cantley LC: The phosphoinositide 3-kinase pathway. *Science* 296:1655–1657, 2002
5. Shepherd PR, Withers DJ, Siddle K: Phosphoinositide 3-kinase: the key switch mechanism in insulin signalling. *Biochem J* 333:471–490, 1998
6. Ueki K, Fruman DA, Brachmann SM, Tseng Y-H, Cantley LC, Kahn CR: Molecular balance between the regulatory and catalytic subunits of phosphoinositide 3-kinase regulates cell signaling and survival. *Mol Cell Biol* 22:965–977, 2002
7. Stokoe D, Stephens LR, Copeland T, Gaffney PRJ, Reese CB, Painter GF, Holmes AB, McCormick F, Hawkins PT: Dual role of phosphatidylinositol-3,4,5-trisphosphate in the activation of protein kinase B. *Science* 277:567–570, 1997
8. Sweeney G, Garg RR, Ceddia RB, Li D, Ishiki M, Somwar R, Foster LJ, Neilsen PO, Prestwich GD, Rudich A, Klip A: Intracellular delivery of phosphatidylinositol (3,4,5)-trisphosphate causes incorporation of glucose transporter 4 into the plasma membrane of muscle and fat cells without increasing glucose uptake. *J Biol Chem* 279:32233–32242, 2004
9. Milburn CC, Deak M, Kelly SM, Price NC, Alessi DR, Van Aalten DM: Binding of phosphatidylinositol 3,4,5-trisphosphate to the pleckstrin homology domain of protein kinase B induces a conformational change. *Biochem J* 375:531–538, 2003
10. Hanada M, Feng J, Hemmings BA: Structure, regulation and function of PKB/AKT: a major therapeutic target. *Biochim Biophys Acta* 1697:3–16, 2004
11. Pesesse X, Deleu S, De Smedt F, Drayer L, Erneux C: Identification of a second SH2-domain-containing protein closely related to the phosphatidylinositol polyphosphate 5-phosphatase SHIP. *Biochem Biophys Res Commun* 239:697–700, 1997
12. Ishihara H, Sasaoka T, Hori H, Wada T, Hirai H, Haruta T, Langlois WJ, Kobayashi M: Molecular cloning of rat SH2-containing inositol phosphatase 2 (SHIP2) and its role in the regulation of insulin signaling. *Biochem Biophys Res Commun* 260:265–272, 1999
13. Clément S, Krause U, Desmedt F, Tanti J-F, Behrends J, Pesesse X, Sasaki T, Penninger J, Doherty M, Malaisse W, Dumont JE, Le Marchand-Brustel Y, Erneux C, Hue L, Schurmans S: The lipid phosphatase SHIP2 controls insulin sensitivity. *Nature* 409:92–97, 2001
14. Kaisaki PJ, Delépine M, Woon PY, Sebag-Montefiore L, Wilder SP, Menzel S, Vionnet N, Marion E, Riveline J-P, Charpentier G, Schurmans S, Levy JC, Lathrop M, Farrall M, Gauguier D: Polymorphisms in type II SH2 domain-containing inositol 5-phosphatase (INPPL1, SHIP2) are associated with physiological abnormalities of the metabolic syndrome. *Diabetes* 53:1900–1904, 2004
15. Marion E, Kaisaki PJ, Pouillon V, Gueydan C, Levy JC, Bodson A, Krzentowski G, Daubresse JC, Mockel J, Behrends J, Servais G, Szpirer C, Kruys V, Gauguier D, Schurmans S: The gene INPPL1, encoding the lipid phosphatase SHIP2, is a candidate for type 2 diabetes in rat and man. *Diabetes* 51:2012–2017, 2002
16. Pesesse X, Moreau C, Drayer AL, Woscholski R, Parker P, Erneux C: The SH2 domain containing inositol 5-phosphatase SHIP2 displays phosphatidylinositol 3,4,5-trisphosphate and inositol 1,3,4,5-tetrakisphosphate 5-phosphatase activity. *FEBS Lett* 437:301–303, 1998
17. Backers K, Blero D, Paternotte N, Zhang J, Erneux C: The termination of PI3K signalling by SHIP1 and SHIP2 inositol 5-phosphatases. *Adv Enzyme Regul* 43:15–28, 2003
18. Wada T, Sasaoka T, Funaki M, Hori H, Murakami S, Ishiki M, Haruta T, Asano T, Ogawa W, Ishihara H, Kobayashi M: Overexpression of SH2-containing inositol phosphatase 2 results in negative regulation of insulin-induced metabolic actions in 3T3–L1 adipocytes via its 5′-phosphatase catalytic activity. *Mol Cell Biol* 21:1633–1646, 2001
19. Sasaoka T, Hori H, Wada T, Ishiki M, Haruta T, Ishihara H, Kobayashi M: SH2-containing inositol phosphatase 2 negatively regulates insulin-induced glycogen synthesis in L6 myotubes. *Diabetologia* 44:1258–1267, 2001
20. Sasaoka T, Wada T, Fukui K, Murakami S, Ishihara H, Suzuki R, Tobe K, Kadowaki T, Kobayashi M: SH2-containing inositol phosphatase 2 predominantly regulates Akt2, and not Akt1, phosphorylation at the plasma membrane in response to insulin in 3T3–L1 adipocytes. *J Biol Chem* 279:14835–14843, 2004
21. Hori H, Sasaoka T, Ishihara H, Wada T, Murakami S, Ishiki M, Kobayashi M: Association of SH2-containing inositol phosphatase 2 with the insulin resistance of diabetic db/db mice. *Diabetes* 51:2387–2394, 2002
22. Murakami S, Sasaoka T, Wada T, Fukui K, Nagira K, Ishihara H, Usui I, Kobayashi M: Impact of Src homology 2-containing inositol 5′-phosphatase 2 on the regulation of insulin signaling leading to protein synthesis in 3T3–L1 adipocytes cultured with excess amino acids. *Endocrinology* 145:3215–3223, 2004
23. Michael MD, Kulkarni RN, Postic C, Previs SF, Shulman GI, Magnuson MA, Kahn CR: Loss of insulin signaling in hepatocytes leads to severe insulin resistance and progressive hepatic dysfunction. *Mol Cell* 6:87–97, 2000
24. Rutter GA: Diabetes: the importance of the liver. *Curr Biol* 10:R736–R738, 2000

25. O'Brien RM, Streeper RS, Ayala JE, Stadelmaier BT, Hornbuckle LA: Insulin-regulated gene expression. *Biochem Soc Trans* 29:552–558, 2001
26. Kubota N, Tobe K, Terauchi Y, Eto K, Yamauchi T, Suzuki R, Tsubamoto Y, Komeda K, Nakano R, Miki H, Satoh S, Sekihara H, Sciacchitano S, Lesniak M, Aizawa S, Nagai R, Kimura S, Akanuma Y, Taylor SI, Kadowaki T: Disruption of insulin receptor substrate 2 causes type 2 diabetes because of liver insulin resistance and lack of compensatory β-cell hyperplasia. *Diabetes* 49:1880–1889, 2000
27. Mithieux G, Daniele N, Payrastre B, Zitoun C: Liver microsomal glucose-6-phosphatase is competitively inhibited by the lipid products of phosphatidylinositol 3-kinase. *J Biol Chem* 273:17–19, 1998
28. Cho H, Mu J, Kim JK, Thorvaldsen JL, Chu Q, Crenshaw EB 3rd, Kaestner KH, Bartolomei MS, Shulman GI, Birnbaum MJ: Insulin resistance and a diabetes mellitus-like syndrome in mice lacking the protein kinase Akt2 (PKBβ). *Science* 292:1728–1731, 2001
29. Barthel A, Schmoll D: Novel concepts in insulin regulation of hepatic gluconeogenesis. *Am J Physiol Endocrinol Metab* 285:E685–E692, 2003
30. Matsumoto M, Ogawa W, Teshigawara K, Inoue H, Miyake K, Sakaue H, Kasuga M: Role of the insulin receptor substrate 1 and phosphatidylinositol 3-kinase signaling pathway in insulin-induced expression of sterol regulatory element–binding protein 1c and glucokinase genes in rat hepatocytes. *Diabetes* 51:1672–1680, 2002
31. Noguchi T, Matsuda T, Tomari Y, Yamada K, Imai E, Wang Z, Ikeda H, Tanaka T: The regulation of gene expression by insulin is differentially impaired in the liver of the genetically obese-hyperglycemic Wistar fatty rat. *FEBS Lett* 328:145–148, 1993
32. Shimano H, Horton JD, Hammer RE, Shimomura I, Brown MS, Goldstein JL: Overproduction of cholesterol and fatty acids causes massive liver enlargement in transgenic mice expressing truncated SREBP-1a. *J Clin Invest* 98:1575–1584, 1996
33. Beale EG, Chrapkiewicz NB, Scoble HA, Metz RJ, Quick DP, Noble RL, Donelson JE, Biemann K, Granner DK: Rat hepatic cytosolic phosphoenolpyruvate carboxykinase (GTP): structures of the protein, messenger RNA, and gene. *J Biol Chem* 260:10748–10760, 1985
34. Shingu R, Nakajima H, Horikawa Y, Hamaguchi T, Yamasaki T, Miyagawa J, Namba M, Hanafusa T, Matsuzawa Y: Expression and distribution of glucose-6-phosphatase catalytic subunit messenger RNA and its changes in the diabetic state. *Res Commun Mol Pathol Pharmacol* 93:13–24, 1996
35. Miyake K, Ogawa W, Matsumoto M, Nakamura T, Sakaue H, Kasuga M: Hyperinsulinemia, glucose intolerance, and dyslipidemia induced by acute inhibition of phosphoinositide 3-kinase signaling in the liver. *J Clin Invest* 110:1483–1491, 2002
36. Jaffe HA, Danel C, Longenecker G, Metzger M, Setoguchi Y, Rosenfeld MA, Gant TW, Thorgeirsson SS, Stratford-Perricaudet LD, Perricaudet M, Pavirani A, Lecocq JP, Crystal RG: Adenovirus-mediated in vivo gene transfer and expression in normal rat liver. *Nat Genet* 1:372–378, 1992
37. Alessi DR, Andjelkovic M, Caudwell B, Cron P, Morrice N, Cohen P, Hemmings BA: Mechanism of activation of protein kinase B by insulin and IGF-1. *EMBO J* 15:6541–6551, 1996
38. Andjelkovic M, Alessi DR, Meier R, Fernandez A, Lamb NJC, Frech M, Cron P, Cohen P, Lucocq JM, Hemmings BA: Role of translocation in the activation and function of protein kinase B. *J Biol Chem* 272:31515–31524, 1997
39. Kobayashi K, Forte TM, Taniguchi S, Ishida BY, Oka K, Chan L: The db/db mouse, a model for diabetic dyslipidemia: molecular characterization and effects of Western diet feeding. *Metabolism* 49:22–31, 2000
40. Shao J, Yamashita H, Qiao L, Friedman JE: Decreased Akt kinase activity and insulin resistance in C57BL/KsJ-Lepr$^{db/db}$ mice. *J Endocrinol* 167:107–115, 2000
41. Sleeman MW, Wortley KE, Lai KM, Gowen LC, Kintner J, Kline WO, Garcia K, Stitt TN, Yancopoulos GD, Wiegand SJ, Glass DJ: Absence of the lipid phosphatase SHIP2 confers resistance to dietary obesity. *Nat Med* 11:199–205, 2005
42. Maehama T, Dixon JE: The tumor suppressor, PTEN/MMAC1, dephosphorylates the lipid second messenger, phosphatidylinositol 3,4,5-trisphosphate. *J Biol Chem* 273:13375–13378, 1998
43. Stiles B, Wang Y, Stahl A, Bassilian S, Lee WP, Kim YJ, Sherwin R, Devaskar S, Lesche R, Magnuson MA, Wu H: Liver-specific deletion of negative regulator Pten results in fatty liver and insulin hypersensitivity. *Proc Natl Acad Sci U S A* 101:2082–2087, 2004
44. Butler M, McKay RA, Popoff IJ, Gaarde WA, Witchell D, Murray SF, Dean NM, Bhanot S, Monia BP: Specific inhibition of PTEN expression reverses hyperglycemia in diabetic mice. *Diabetes* 51:1028–1034, 2002
45. Postic C, Shiota M, Magnuson MA: Cell-specific roles of glucokinase in glucose homeostasis. *Recent Prog Horm Res* 56:195–217, 2001
46. Horton JD, Shimomura I, Ikemoto S, Bashmakov Y, Hammer RE: Overexpression of sterol regulatory element-binding protein-1a in mouse adipose tissue produces adipocyte hypertrophy, increased fatty acid secretion, and fatty liver. *J Biol Chem* 278:36652–36660, 2003
47. Vuguin P, Raab E, Liu B, Barzilai N, Simmons R: Hepatic insulin resistance precedes the development of diabetes in a model of intrauterine growth retardation. *Diabetes* 53:2617–2622, 2004
48. Shimomura I, Matsuda M, Hammer RE, Bashmakov Y, Brown MS, Goldstein JL: Decreased IRS-2 and increased SREBP-1c lead to mixed insulin resistance and sensitivity in livers of lipodystrophic and ob/ob mice. *Mol Cell* 6:77–86, 2000
49. Seoane J, Trinh K, O'Doherty RM, Gómez-Foix AM, Lange AJ, Newgard CB, Guinovart JJ: Metabolic impact of adenovirus-mediated overexpression of the glucose-6-phosphatase catalytic subunit in hepatocytes. *J Biol Chem* 272:26972–26977, 1997
50. Sun Y, Liu S, Ferguson S, Wang L, Klepcyk P, Yun JS, Friedman JE: Phosphoenolpyruvate carboxykinase overexpression selectively attenuates insulin signaling and hepatic insulin sensitivity in transgenic mice. *J Biol Chem* 277:23301–23307, 2002

GLIA 52:47–52 (2005)

Evidence for Creatine Biosynthesis in Müller Glia

TOSHIHISA NAKASHIMA,[1] MASATOSHI TOMI,[1] MASANORI TACHIKAWA,[2] MASAHIKO WATANABE,[3] TETSUYA TERASAKI,[2,4,5] AND KEN-ICHI HOSOYA[1]*
[1]*Faculty of Pharmaceutical Sciences, Toyama Medical and Pharmaceutical University, Toyama, Japan*
[2]*Department of Molecular Biopharmacy and Genetics, Graduate School of Pharmaceutical Sciences, Tohoku University, Sendai, Japan*
[3]*Department of Anatomy, Hokkaido University School of Medicine, Sapporo, Japan*
[4]*New Industry Creation Hatchery Center, Tohoku University, Sendai, Japan*
[5]*SORST of the Japan Science and Technology Agency (JST), Kawaguchi, Saitama, Japan*

KEY WORDS
GAMT; rat retina; immunohistochemistry; glutamine synthetase; Müller cell line

ABSTRACT
In high-energy metabolic tissues like the retina, creatine may play an important role in energy storage and in transmission of phosphate-bound energy substrates. To prove this, we investigated creatine synthesis in Müller glia. We also characterized the localization of the creatine synthetic enzyme, S-adenosyl-L-methionine:N-guanidinoacetate methyltransferase (GAMT) in the retina. Reverse transcription-polymerase chain reaction analysis revealed that L-arginine:glycine amidinotransferase and GAMT mRNAs were expressed in the retina and the Müller cell line, TR-MUL5. [^{14}C]Creatine was detected after incubation of isolated rat retina or TR-MUL5 cells with [^{14}C]glycine, L-arginine and L-methionine, suggesting creatine synthesis in Müller glia. Western blot analysis also revealed expression of GAMT protein in the rat retina and TR-MUL5 cells. Furthermore, confocal immunofluorescent microscopy of dual-labeled rat retinal sections demonstrated co-localization of GAMT with glutamine synthetase. Taken together, the results of the present study indicate creatine synthesis in Müller glia, implying an important role of creatine in energy metabolism in the retina.

INTRODUCTION

The creatine/phosphocreatine system plays a pivotal role in the maintenance of ATP homeostasis in highly energy-demanding tissues such as the brain and skeletal muscles (Wyss and Kaddurah-Daouk, 2000). High levels of creatine in the chick retina (3 mM) and in the photoreceptor cells (10–15 mM) suggest that the creatine/phosphocreatine system may also be significant in the retina, where photoreceptor cells require a large amount of metabolic energy for phototransduction maintained by ionic gradients across the plasma membrane (Hall and Kühn, 1986; Wallimann et al., 1986; Sather and Detwiler, 1987). In fact, it has been shown that the gyrate atrophy (GA) of the choroids and retina is characterized by hyperornithinemia and hypocreatinemia, implying that excessive ornithine leads to chorioretinal degeneration through suspension of creatine synthesis (Sipila et al., 1992). The high level of creatine in the retina is maintained by a supply from the circulating blood through the blood-retinal barrier (BRB) or local biosynthesis in the retina. We have recently shown the presence of a creatine transporter (CRT) at the rat inner blood-retinal barrier (inner BRB) (Nakashima et al., 2004). A deficiency of creatine transporters in humans results in mental retardation, seizures and central hypotonia (Schulze, 2003). However, retinal dysfunction or degeneration rarely develops in these patients, suggesting that transportation of creatine from the circulating blood does not play an important role in sustaining the creatine/phosphocreatine system in the retina. We now hypothesize that creatine can be synthesized locally in the retina. Although creatine is mainly synthesized in other organs, such as the kidney, liver, and pancreas, creatine is also synthesized in the brain (Defalco and Davies, 1961; Wyss and Kaddurah-Daouk, 2000). In the central nervous system, it has been shown that S-adenosyl-L-methionine:N-guanidinoacetate methyltransferase (GAMT), a key enzyme for creatine synthesis, is highly and exclusively expressed in glial cells, including oligodendrocytes, olfactory ensheathing glia, and astrocytes, raising the possibility that creatine is also synthesized in Müller glia, the most predominant glia in the retina (Dringen et al., 1998; Tachikawa et al., 2004). Although GAMT activities have been demonstrated in the retina of various species including rats, there have been no investigations of the cellular system for creatine biosynthesis in the retina (Mardashchev, 1975). Using high-performance liquid chromatography (HPLC), reverse transcription-polymerase chain reaction (RT-PCR), Western blot analysis, and confocal immunofluorescence imaging, we report that creatine is synthesized in Müller glia.

Grant sponsor: Japan Society for the Promotion of Science; Grant sponsor: Ministry of Health, Labor, and Welfare, Japan.

Masanori Tachikawa is currently at the Faculty of Pharmaceutical Sciences, Toyama Medical and Pharmaceutical University, Toyama, Japan.

*Correspondence to: Ken-ichi Hosoya, Faculty of Pharmaceutical Sciences, Toyama Medical and Pharmaceutical University, 2630 Sugitani, Toyama 930-0194, Japan. E-mail: hosoyak@ms.toyama-mpu.ac.jp

Received 8 November 2004; Accepted 7 March 2005

DOI 10.1002/glia.20222

Published online 12 May 2005 in Wiley InterScience (www.interscience.wiley.com).

MATERIALS AND METHODS

Animals

Male Wistar rats (250–300 g), male ddY mice (25–30 g), and female New Zealand White rabbits (3.1–3.5 kg) were purchased from SLC (Shizuoka, Japan). The investigations using animals described in this report conformed to the provisions of the Animal Care Committee, Toyama Medical and Pharmaceutical University (#2003-48), and the ARVO Statement on the Use of Animals in Ophthalmic and Vision Research.

Reagents

[1-^{14}C]D-Mannitol ([^{14}C]D-mannitol, 53.7 mCi/mmol), and [U-^{14}C]glycine ([^{14}C]glycine, 101 mCi/mmol) were purchased from Amersham Biosciences (Buckinghamshire, UK); L-[2,3,4-^{3}H] L-arginine HCl ([^{3}H] L-arginine, 40 Ci/mmol) was from Perkin-Elmer Life Sciences (Boston, MA); [4-^{14}C]creatine ([^{14}C]creatine, 55 mCi/mmol) was from American Radiolabeled Chemicals (St. Louis, MO). All other chemicals were of reagent grade and available commercially.

Cell Culture

TR-MUL5 cells, which had been established and characterized previously (Tomi et al., 2003), were used as an in vitro model of Müller glia to examine expression of creatine biosynthetic enzymes and biosynthesis of creatine. TR-MUL5 cells (passages 15–25) were cultured at 33°C in Dulbecco's modified Eagle's medium (Nissui Pharmaceuticals, Tokyo, Japan) under 5% CO_2/air. The permissive temperature for the culture of TR-MUL5 cells is 33°C, due to the expression of temperature-sensitive large T-antigen (Tomi et al., 2003; Hosoya and Tomi, 2005). For the biosynthesis and uptake studies, cells (3×10^5 cells/cm^2) were cultured at 33°C for 24 h on a 24-well tissue culture plate (BD Biosciences, Bedford, MA).

An Ex Vivo Rat Retinal Preparation

Retinal isolation and ex vivo studies were performed using a modification of the procedure described by Izumi et al. (1995). Briefly, under deep pentobarbital anesthesia (100 mg/kg body weight, i.p.), the eyes of Wistar rats were enucleated, and retinas were dissected in ice-cold phosphate-buffered saline (PBS). Freshly extirpated retinas were placed on the insert of a Transwell^{TM} (12-mm diameter, 0.4-μm pore size, polycarbonate membranes) (Corning, New York, NY) and pre-incubated in 1 ml minimal medium (MM; 110 mM NaCl, 44 mM $NaHCO_3$, 1.8 mM $CaCl_2$, 5.4 mM KCl, 0.8 mM $MgSO_4$, 0.92 mM NaH_2PO_4, containing 10% dialyzed fetal bovine serum, 1 mM L-methionine, and 1 mM L-arginine, pH 7.4) (Dringen et al., 1998), which was equilibrated with 5% CO_2/95% O_2, at 30°C for 1 h.

Creatine Biosynthesis Study

After pre-incubation of isolated retinas, the inserts were transferred to other wells and were incubated in 1 ml MM containing 1 μCi [^{14}C]glycine (10 μM) at 37°C in dark and a humidified atmosphere of 5% CO_2/air for 24 h. TR-MUL5 cells were washed three times with 1 ml MM and then incubated in 1 ml MM containing 1 μCi [^{14}C]glycine (10 μM) at 33°C in a humidified atmosphere of 5% CO_2/air for 24 h. After a 24 h-incubation, retinas and cells were washed with ice-cold PBS and homogenized in ice-cold 70% methanol. After centrifugation at 4°C and 12,000*g* for 5 min, an aliquot of the samples was subjected to HPLC using a system equipped with a 4.6 × 150-mm Inertsil ODS-3 column (GL Sciences, Tokyo, Japan). The mobile phase consisted of 99.5% 5 mM 1-octanesulfonic acid and 30 mM K_2HPO_4–0.5% methanol (pH 2.5) at a flow rate of 0.5 ml/min. The eluent was collected in vials, and the radioactivity in each fraction was determined by liquid scintillation counting.

RT-PCR Analysis

Total cellular RNA was prepared from PBS-washed cells using the RNeasy Mini Kit (Qiagen, Hilden, Germany). Single-strand cDNA was made from 1 μg total RNA by reverse transcription (RT) using oligo dT primer. The polymerase chain reaction (PCR) was performed using a gene amplification system (GeneAmp PCR system 9700; PE-Applied Biosystems, Foster City, CA) with GAMT and L-arginine:glycine amidinotransferase (AGAT) through 40 cycles of 94°C for 30 s, 62°C for 1 min, and 72°C for 2 min. The sequences of the specific primers were as follows: sense, 5′-TCT GAC ACG CAC CTG CAG ATC C-3′; antisense, 5′-GCA TAG TAG CGG CAG TCG GCT G-3′ for rat GAMT (GenBank accession number X08056); sense, 5′-TAA CAG GAT GGG TGC AGC GAA CT-3′; antisense, 5′-GGT CAT ACA GTT CGT CAG CCA T-3′ for rat arginine/glycine aminotransferase (AGAT) (GenBank accession number U07971). The PCR products were separated by electrophoresis on an agarose gel in the presence of ethidium bromide and visualized under ultraviolet (UV) light. The molecular identity of the resultant product was confirmed by sequence analysis using a DNA sequencer (Prism 310; PE-Applied Biosystems).

Western Blot Analysis

Tissue and cell lysates of adult mouse brain, adult rat brain, retina, liver, and TR-MUL5 cells were prepared in sample buffer consisting of 5% sodium dodecyl sulfate (SDS), 50 mM Tris-HCl (pH 6.8), 10% glycerol, 6% 2-mercaptoethanol, 0.01% bromophenol blue, and 0.1% protease-inhibitor cocktail (Sigma, St. Louis, MO). To prepare total protein fractions, the lysates were centrifuged at 8,000 g and 4°C for 10 min, and the super-

natants were collected. The protein concentration was measured using a kit (DC, Bio-Rad, Hercules, CA). The protein was electrophoresed on a 12% SDS-polyacrylamide gel and electrotransferred to a polyvinylidene difluoride (PVDF) membrane (Bio-Rad). The blotted membranes were incubated with affinity-purified guinea pig polyclonal antibody against mouse GAMT (Tachikawa et al., 2004) at 1.5 μg/ml as the primary antibody using blocking agent solution (Block Ace; Dainihon Pharmaceutical, Osaka, Japan). There was apparently sufficient antibody cross-reactivity between mouse and rat GAMT (Fig. 3). The membranes were subsequently incubated with horseradish peroxidase conjugated donkey anti-guinea pig IgG antibody as the secondary antibody. The bands were visualized with an enhanced chemiluminescence kit (ECL; Amersham Biosciences).

Immunohistochemistry

Under deep pentobarbital anesthesia, Wistar rats were perfused transcardially with 4% paraformaldehyde in 0.1 M sodium phosphate buffer (pH 7.2). The retina was embedded in paraffin wax after dehydration using graded alcohols, and paraffin sections (5-μm thickness) were prepared with a sliding microtome (SM2000R; Leica Microsystems, Wetzlar, Germany). Before immunohistochemical investigation, the paraffin sections were digested with pepsin (1 mg/ml in 0.2 M HCl, Dako, Carpinteria, CA) for 5 min at 37°C to retrieve antigens. For immunofluorescence, sections were incubated at room temperature with 10% normal goat serum (NGS) for 30 min, guinea pig anti-GAMT antibody 2 μg/ml singly or in combination with rabbit anti-glutamine synthetase antibody (1 μg/ml) overnight, and subsequently incubated with FITC- or Cy3-conjugated secondary antibodies for 2 h (Jackson ImmunoResearch, West Grove, PA). Polyclonal antibody to glutamine synthetase (GS) was raised against amino acid residues 344–373 of mouse GS (GenBank accession number AY044241). The polypeptides were synthesized and linked to maleimide-activated keyhole limpet hemocyanin (KLH; Pierce, Rockford, IL). The KLH-linked polypeptides (200 μg/injection) were emulsified by mixing with an equal volume of Freund's adjuvant (Difco, Detroit, MI) and injected subcutaneously into female New Zealand White rabbits at intervals of 2 weeks. Two weeks after the sixth injection, affinity-purified antibodies were prepared, first using protein G-Sepharose (Amersham Biosciences) and then using antigen polypeptides free of KLH coupled to cyanogen bromide-activated Sepharose 4B (Amersham Biosciences). Western blot analysis using mouse brain, rat brain, and rat retina extracts showed that rabbit anti-GS antibody strongly recognized a single protein band at 44 kDa (data not shown), the size of which is consistent with that of a previous report (Shen et al., 2004). Photographs were taken with a confocal laser scanning microscope (Fluoview, Olympus, Tokyo, Japan).

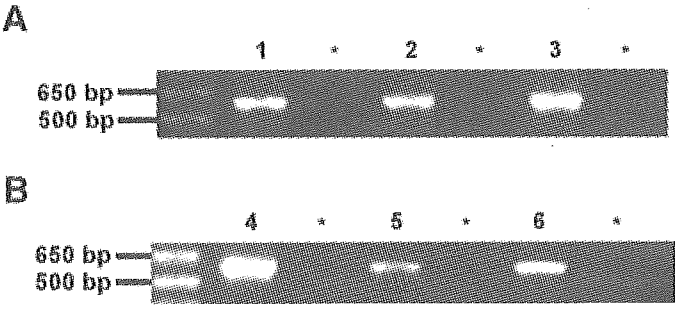

Fig. 1. Reverse transcription-polymerase chain reaction (RT-PCR) analysis of GAMT (**A**) and AGAT (**B**) in the rat retina and TR-MUL5 cells. **Lane 1**, rat liver; **lanes 2 and 5**, rat retina; **lanes 3 and 6**, TR-MUL5 cells; **lane 4**, rat brain; asterisk, in the absence of reverse transcriptase for the respective left-hand lane. Rat liver and brain were used as a positive control for GAMT and AGAT, respectively.

RESULTS

Expression of GAMT and AGAT mRNAs in the Rat Retina and TR-MUL5 Cells

To examine the expression of creatine biosynthetic enzymes in the retina and Müller glia, we performed RT-PCR analysis, using total RNA isolated from the rat retina and Müller cell line, TR-MUL5, and specific primers for rat GAMT and AGAT (Fig. 1). Using the rat liver (lane 1) and brain (lane 4) as positive controls, GAMT and AGAT cDNAs were successfully amplified at 584 and 591 bp, respectively, in the retina (lanes 2 and 5) and TR-MUL5 cells (lanes 3 and 6). These results indicate that creatine biosynthetic enzymes are transcribed in the rat retina and TR-MUL5 cells.

Creatine Biosynthesis in the Rat Retina and TR-MUL5 Cells

Creatine is synthesized from glycine and -L-arginine, and two carbons of creatine are derived from glycine. Thus, we used [^{14}C]glycine to determine whether creatine is biosynthesized by detecting [^{14}C]creatine using HPLC. Firstly, the uptake of [^{14}C]glycine and [^{3}H]-L-arginine by TR-MUL5 cells was examined. The initial uptake rate of [^{14}C]glycine and [^{3}H]L-arginine in TR-MUL5 cells was 7.29 μl/(min · mg protein) and 28.3 μl/(min · mg protein), which were 14.5-fold and 56.4-fold greater, respectively, than that of [^{3}H]-D-mannitol (0.502 μl/(min · g protein)) (data not shown). This finding suggests that the precursor amino acids, glycine and L-arginine, are taken up by TR-MUL5 cells at much greater rates than by nonspecific adsorption or passive diffusion.

Figure 2 shows the HPLC chromatograms of [^{14}C]glycine (Fig. 2A), [^{14}C]creatine (Fig. 2B), and samples of isolated retina (Fig. 2C) and TR-MUL5 cells (Fig. 2D). After 24-h incubation of isolated retinas and TR-MUL5 cells with [^{14}C]glycine, the peaks of [^{14}C]creatine appeared at the same time point both in isolated retina

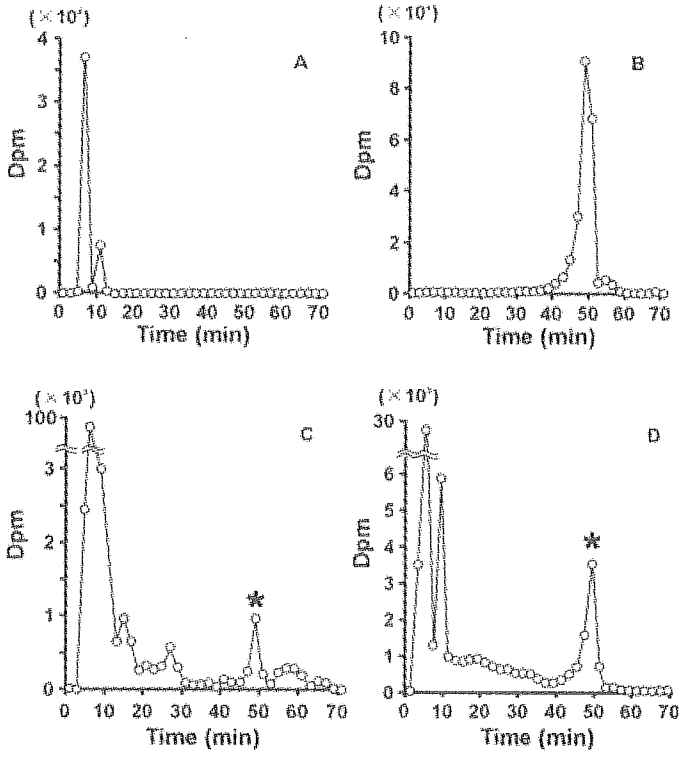

Fig. 2. Typical high-performance liquid chromatography (HPLC) of samples of isolated rat retina (**C**) and TR-MUL5 cells (**D**). The isolated retinas and TR-MUL5 cells were incubated in medium containing 1 μCi [^{14}C]glycine (10 μM), L-arginine (1 mM), and L-methionine (1 mM) for 24 h at 37 and 33°C, respectively. The asterisk indicates [^{14}C]-labeled creatine synthesized from [^{14}C]glycine in the rat retinas and TR-MUL5 cells. **A,B:** Typical chromatograms of [^{14}C]glycine and [^{14}C]creatine, respectively.

(Fig. 2C) and TR-MUL5 cells (Fig. 2D), suggesting creatine biosynthesis in the rat retina and Müller glia.

Preferential Distribution of GAMT in Müller Glia of the Rat Retina

We then examined the distribution of GAMT in the rat retina by confocal immunofluorescence microscopy. Although anti-GAMT antibody was raised against amino acids residues 1–236 of mouse GAMT (Tachikawa et al., 2004), sufficient cross-reactivity between mouse and rat was found by Western blot analysis (Fig. 3). Similarly to the mouse brain (lane 1), rat liver (lane 2), and rat brain (lane 3), a band at 27 kDa was observed in the rat retina (lane 4) and TR-MUL5 cells (lane 5).

Using double immunofluorescence, intense GAMT immunoreactivity was found to be distributed in fibrous structures, which projected radially throughout the retina from the inner to the outer limiting membrane (Fig. 4A). The fibrous structures extensively overlapped with GS, a specific marker for glial cells in the retina (Fig. 4B–D). GAMT was also detected in GS-positive Müller cell bodies (Fig. 4C, arrowheads), and Müller cells and astrocytes in the ganglion cell layer (Fig. 4D). In addition, tiny puncta with low to moderate GAMT

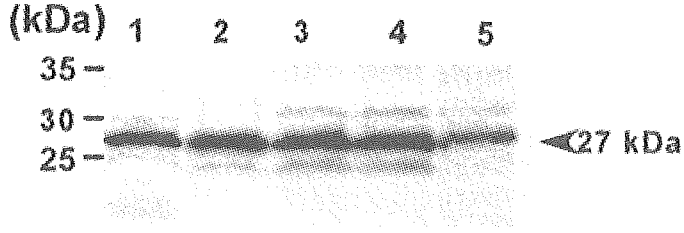

Fig. 3. Western blot analysis of rat GAMT using anti-mouse GAMT antibody in the rat retina and TR-MUL5 cells. **Lane 1**, mouse brain; **lane 2**, rat liver; **lane 3**, rat brain; **lane 4**, rat retina; **lane 5**, TR-MUL5 cells. The single band at 27 kDa in the rat retina and TR-MUL5 cells has the same molecular weight as that in the mouse brain, rat liver, and rat brain used as positive controls.

intensity were also detected between the fibrous structures, but they were negative for glutamine synthetase (Figs. 4B-D). Such characteristic immunostaining was abolished when preimmune guinea pig immunoglobulin or primary antibody preabsorbed with GAMT antigen peptides (100 μg/ml; data not shown) was used. These features indicate that GAMT is exclusively expressed in Müller glia with additional expression in neuronal cells or some other glial cells at low to moderate levels.

DISCUSSION

The present study demonstrates the expression of creatine biosynthetic enzymes and creatine biosynthesis in the rat retina and TR-MUL5 cells. Moreover, there is preferential localization of GAMT in Müller cells of the rat retina. This is the first direct evidence of creatine biosynthesis in Müller cells of the retina.

Glycine and L-arginine, which are precursor amino acids for creatine biosynthesis, are thought to be synthesized de novo in the cells. However, there is no report regarding de novo synthesis of both amino acids in Müller cells. In TR-MUL5 cells, uptake rate of glycine and L-arginine was much faster than that of D-mannitol, suggesting that some neutral and cationic amino acid transporters actively transport these amino acids. This evidence is consistent with previous reports (Pow and Crook, 1997; Gadea et al., 1999; Reye et al., 2001). Glycine transport appears to take place via Glyt-1 and/or system A in the primary cultured Müller cells (Gadea et al., 1999; Reye et al., 2001). L-Arginine transport may occur in retinal Müller glia (Pow and Crook, 1997). In contrast, Reye et al. (2001) reported that Glyt-1 is not expressed in Müller glia in vivo. The lack of agreement between the expression of glycine transporter in the cultured Müller cells and Müller glia in vivo needs an explanation. Conceivably, Glyt-1 is up-regulated in cultured Müller cells. Although further studies are needed to identify glycine and L-arginine transporters in Müller glia in vivo, TR-MUL5 cells have the ability to take up glycine and L-arginine. The expression of AGAT and GAMT mRNA in the retina and TR-MUL5 cells suggests that creatine biosynthesis takes place in Müller glia (Fig. 1).

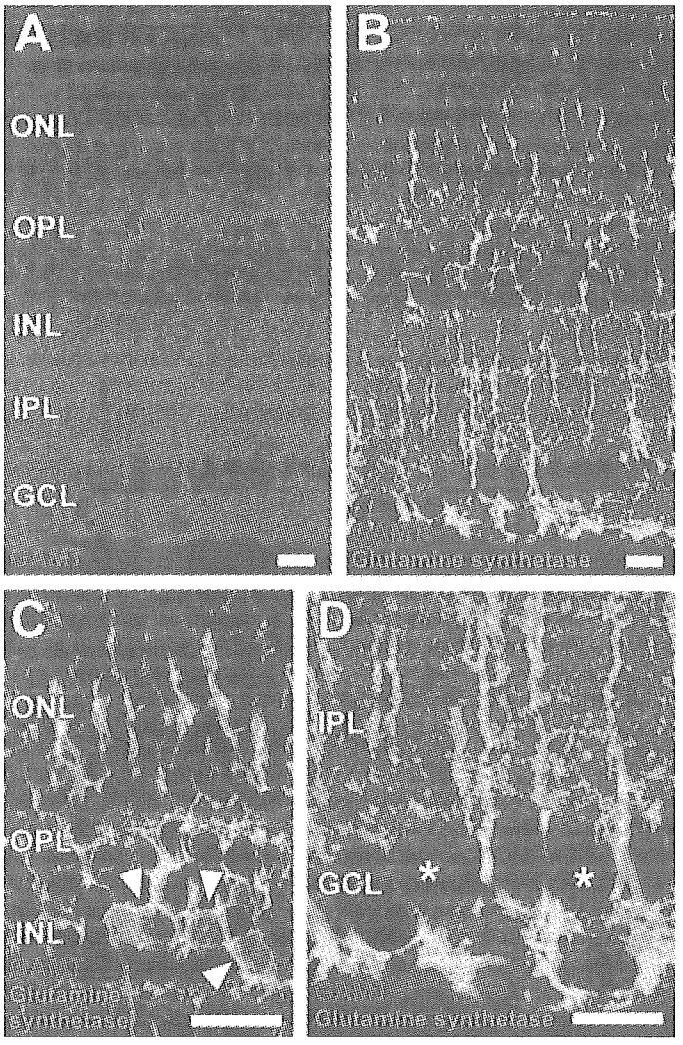

Fig. 4. Confocal immunofluorescence microscope images of single (**A**) or dual-labeled (**B–D**) rat retinal sections. The retinal sections were stained with anti-GAMT antibody (red) singly (A) or in combination with anti-glutamine synthetase antibody (green), a marker for glial cells (B–D). Arrowheads (C) and asterisks (D) indicate Müller cell bodies and ganglion cell bodies, respectively. ONL, outer nuclear layer; OPL, outer plexiform layer; INL, inner nuclear layer; IPL, inner plexiform layer; GCL, ganglion cell layer. Scale bars = 10 μm.

Indeed, [^{14}C]creatine was identified in the isolated retina and TR-MUL5 cells after a 24 h-incubation with [^{14}C]glycine added to the culture medium (Fig. 2). Moreover, confocal immunofluorescence microscopy with rat retinal sections demonstrated that GAMT is preferentially localized in GS-positive retinal cells, i.e., Müller cells and astrocytes (Fig. 4). Astrocytes are largely confined to the nerve fiber layer of the retina (Pfeiffer-Guglielmi et al., 2004) and GS-positive cells are mainly seen in profile, with their endfeet within the nerve fiber layer and their cell bodies in the inner nuclear layer (Fig. 4). These features suggest that creatine biosynthesis is mainly responsible for Müller cells and partly for astrocytes in the rat retina. These findings support the hypothesis that creatine is largely biosynthesized in Müller glia.

The role and fate of creatine synthesized in retinal Müller cells remain unknown. We assume that synthesized creatine is not only used by Müller cells, but is also supplied to other cells, most likely photoreceptor cells, to maintain ATP homeostasis. Visual transduction processes in photoreceptor cells involve many ATP-requiring reactions, such as ATP-dependent regeneration and phosphorylation of the rhodopsin photopigment by rhodopsin kinase, ATP-dependent Na^+, K^+-ATPase of the photoreceptor cell membrane, ATP-dependent phosphotidylinositol/inositol trisphosphate-signaling pathway, and ATP-requiring neurotransmitter synthesis (Koenekoop, 2004). To meet this enormous requirement, photoreceptor cells are thought to generate 34 ATP via the tricarboxylic acid (TCA) cycle rather than from glycolysis using 2 molecules of lactate supplied from local Müller glia (Poitry-Yamate et al., 1995; Magistretti et al., 1999). Since the rate of ATP generation by the creatine/phosphocreatine shuttle system is 10-fold faster than that by oxidative phosphorylation and glycolysis (Wallimann et al., 1992), the creatine/phosphocreatine shuttle system may play a pivotal role in energy storage and regeneration of ATP in photoreceptor cells. In support of this notion, the creatine concentration in chicken photoreceptor cells is as high as 10–15 mM (Wallimann et al., 1986). Interestingly, as far as this point is concerned, creatine kinases are also more concentrated in photoreceptor cells compared with other cells in the chicken retina (Wallimann et al., 1986). Despite the abundance of creatine and creatine kinases, we observed little GAMT immunoreactivity in photoreceptor cells located in the outer nuclear layer, but, instead, intense GAMT immunoreactivity in GS-positive Müller cells (Fig. 4). Therefore, it appears likely that creatine enriched in photoreceptor cells is derived, at least in part, from local Müller glia, like lactate and amino acids which are assumed to be shuttled between Müller cells and photoreceptor cells (Poitry-Yamate et al., 1995; Rauen and Wiessner, 2000). Bearing in mind the fact that creatine is also supplied from the circulating blood via CRT at the inner BRB (Nakashima et al., 2004), the creatine concentration in photoreceptor cells may be controlled by a dual system of creatine supply, i.e., supplies from the local retinal glial cells and capillaries. As far as this novel idea is concerned, there is no report of retinal dysfunction in patients with CRT deficiency. However, it can be explained by creatine synthesis and supply by Müller glia. In contrast, chorioretinal degeneration in patients with GA can be ascribed both to a reduced creatine supply from the circulating blood and a disrupted supply from local Müller glia due to inhibition of creatine biosynthesis by hyperornithinemia in the whole body (Sipila et al., 1980).

The creatine uptake system in photoreceptor cells has not yet been identified. Jones (1995) reported identification and localization of CRT in bovine retina by in situ hybridization showing that CRT mRNA was expressed in all cell types in the retina, whereas CRT mRNA was absent in photoreceptor cells. Although further studies are needed to identify the creatine transport system(s)

in photoreceptor cells, creatine supply to photoreceptor cells from local Müller glia might take place in patients with CRT deficiency.

We studied creatine biosynthesis using albino Wistar rats. Although the retina in albino rats is likely stressed by exposing light compared with that in pigmented rats, we do not think that the creatine biosynthesis in the isolated and dark-adapted (i.e., incubated for 24 h under dark) retinas is influenced by light-induced stress. Moreover, Blaszczyk et al. (2004) reported that the concentrations of γ-aminobutyric acid, L-glutamic acid, and L-serine in the isolated retina of pigmented Long Evans rats are not very largely different from those found in albino Wistar rats.

We provide evidence, for the first time, that creatine is preferentially biosynthesized in Müller cells of the retina. Our current and previous findings offer important information that will increase our understanding of the mechanism of creatine supply and creatine kinetics in the retina and of creatine supplementation in patients with creatine deficiency syndromes.

ACKNOWLEDGMENTS

The authors thank Dr. K. Katayama (Toyama Medical and Pharmaceutical University) for valuable discussions and Dr. D. Jack and Dr. K.J. Kim (University of Southern California) for critical reading of the manuscript. This study was supported, in part, by a Grant-in-Aid for Scientific Research from the Japan Society for the Promotion of Science and a grant for Research on Sensory and Communicative Disorders by the Ministry of Health, Labor, and Welfare, Japan.

REFERENCES

Blaszczyk WM, Straub H, Distler C. 2004. GABA content in the retina of pigmented and albino rats. NeuroReport 15:1141–1144.

Defalco AJ, Davies RK. 1961. The synthesis of creatine by the brain of the intact rat. J Neurochem 7:308–312.

Dringen R, Verleysdonk S, Hamprecht B, Willker W, Leibfritz D, Brand A. 1998. Metabolism of glycine in primary astroglial cells: synthesis of creatine, serine, and glutathione. J Neurochem 70:835–840.

Gadea A, Lopez E, Lopez-Colome AM. 1999. Characterization of glycine transport in cultured Müller glial cells from the retina. Glia 26:273–279.

Hall SW, Kühn H. 1986. Purification and properties of guanylate kinase from bovine retinas and rod outer segments. Eur J Biochem 161:551–556.

Hosoya K, Tomi M. 2005. Advances in the cell biology of transport via the inner blood-retinal barrier: establishment of cell lines and transport functions. Biol Pharm Bull 28:1–8.

Izumi Y, Benz AM, Kurby CO, Labruyere J, Zorumski CF, Price MT, Olney JW. 1995. An ex vivo rat retinal preparation for excitotoxicity studies. J Neurosci Methods 60:219–225.

Jones EM. 1995. Na^+- and Cl^--dependent neurotransmitter transporters in bovine retina: identification and localization by in situ hybridization histochemistry. Vis Neurosci 12:1135–1142.

Koenekoop RK. 2004. An overview of Leber congenital amaurosis: a model to understand human retinal development. Surv Ophthalmol 49:379–398.

Magistretti PJ, Pellerin L, Rothman DL, Shulman RG. 1999. Energy on demand. Science 283:496–497.

Mardashchev SR. 1975. Guanidinoacetate-N-methyltransferase: location in mammalian retina and rat Harderian gland. Biokhimiia 40:353–357.

Nakashima T, Tomi M, Katayama K, Tachikawa M, Watanabe M, Terasaki T, Hosoya K. 2004. Blood-to-retina transport of creatine via creatine transporter (CRT) at the rat inner blood-retinal barrier. J Neurochem 89:1454–1461.

Pfeiffer-Guglielmi B, Francke M, Reichenbach A, Fleckenstein B, Jung G, Hamprecht B. 2004. Glycogen phosphorylase isozyme pattern in mammalian retinal Müller (glial) cells and in astrocytes of retina and optic nerve. Glia 49:84–95.

Poitry-Yamate CL, Poitry S, Tsacopoulos M. 1995. Lactate released by Müller glial cells is metabolized by photoreceptors from mammalian retina. J Neurosci 15:5179–5191.

Pow DV, Crook DK. 1997. Immunocytochemical analysis of the transport of arginine analogues into nitrergic neurons and other cells in the retina and pituitary. Cell Tissue Res 290:501–514.

Reye P, Penfold P, Pow DV. 2001. Glyt-1 expression in cultured human Müller cells and intact retinae. Glia 34:311–315.

Rauen T, Wiessner M. 2000. Fine tuning of glutamate uptake and degradation in glial cells: common transcriptional regulation of GLAST1 and GS. Neurochem Int 37:179–189.

Sather WA, Detwiler PB. 1987. Intracellular biochemical manipulation of phototransduction in detached rod outer segments. Proc Natl Acad Sci USA 84:9290–9294.

Schulze A. 2003. Creatine deficiency syndromes. Mol Cell Biochem 244:143–150.

Shen F, Chen B, Danias J, Lee KC, Lee H, Su Y, Podos SM, Mittag TW. 2004. Glutamate-induced glutamine synthetase expression in retinal Müller cells after short-term ocular hypertension in the rat. Invest Ophthalmol Vis Sci 45:3107–3112.

Sipila I, Simell O, Arjomaa P. 1980. Gyrate atrophy of the choroid and retina with hyperornithinemia. Deficient formation of guanidinoacetic acid from arginine. J Clin Invest 66:684–687.

Sipila I, Valle D, Brusilow S. 1992. Low guanidinoacetic acid and creatine concentration in gyrate atrophy of the choroids and retina (GA). In: De Deyn PP, Marescau B, Stalon V, Qureshi IA, editors. Guanidino compounds in biology and medicine. London: John Libbey. p 379–383.

Tachikawa M, Fukaya M, Terasaki T, Ohtsuki S, Watanabe M. 2004. Distinct cellular expressions of creatine synthetic enzyme GAMT and creatine kinases uCK-Mi and CK-B suggest a novel neuron-glial relationship for brain energy homeostasis. Eur J Neurosci 20:144–160.

Tomi M, Funaki T, Abukawa H, Katayama K, Kondo T, Ohtsuki S, Ueda M, Obinata M, Terasaki T, Hosoya K. 2003. Expression and regulation of L-cystine transporter, system xc^-, in the newly developed rat retinal Müller cell line (TR-MUL). Glia 43:208–217.

Wallimann T, Wegmann G, Moser H, Huber R, Eppenberger HM. 1986. High content of creatine kinase in chicken retina: compartmentalized localization of creatine kinase isoenzymes in photoreceptor cells. Proc Natl Acad Sci USA 83:3816–3819.

Wallimann T, Wyss M, Brdiczka D, Nicolay K, Eppenberger HM. 1992. Intracellular compartmentation, structure and function of creatine kinase isoenzymes in tissues with high and fluctuating energy demands: the "phosphocreatine circuit" for cellular energy homeostasis. Biochem J 281:21–40.

Wyss M, Kaddurah-Daouk R. 2000. Creatine and creatinine metabolism. Physiol Rev 80:1107–1213.

Increased JNK Phosphorylation and Oxidative Stress in Response to Increased Glucose Flux through Increased GLUT1 Expression in Rat Retinal Endothelial Cells

Jie Zhou,[1] *Baljit K. Deo,*[1] *Kenichi Hosoya,*[2] *Tetsuya Terasaki,*[3] *Irina G. Obrosova,*[4] *Frank C. Brosius, III,*[1,5,6] *and Arno K. Kumagai*[1,6]

Purpose. To investigate whether increased glucose flux through increased glucose transporter1 (GLUT1) expression results in increased oxidative stress and increased c-jun N-terminal kinase (JNK) phosphorylation.

Methods. GLUT1-overexpressing cells were established using a rat retinal endothelial cell line. The intracellular reactive oxygen species was detected by the oxidation of 5- (and -6)-chloromethyl-2′,7′-dichlorodihydrofluorescein diacetate, acetyl ester (CM-H2-DCFDA). Western blot was performed to determine JNK phosphorylation and lipid peroxidation. Differentially expressed genes were detected by cDNA microarray analysis and confirmed by Northern blot analysis.

Results. Clones overexpressing GLUT1 showed an approximate four- to eightfold increase in GLUT1 expression and a 44% increase in intracellular glucose concentrations. GLUT1-overexpressing cells had a 80% increase in DCF fluorescence and increased lipid peroxidation, as well as increased JNK phosphorylation. Analysis of differentially expressed genes in GLUT1-overexpressing cells showed increased expression of JNK interacting protein (JIP)-1, a scaffold protein necessary for JNK activation. Northern blot analysis confirmed upregulation of JIP-1. Immunoprecipitation showed that phosphorylated JNK, but not total JNK, coimmunoprecipitated with JIP-1 protein. At the cellular level, JIP-1 was predominantly localized in cytoplasm, especially in the perinuclear area in retinal endothelial cells.

Conclusions. GLUT1 overexpression and increased glucose flux result in increased oxidative stress and JNK phosphorylation in immortalized rat retinal endothelial cells. Further studies are needed to understand molecular events after increased glucose flux in retinal endothelial cells and the relation between increased oxidative stress and JNK phosphorylation. (*Invest Ophthalmol Vis Sci.* 2005;46:3403–3410) DOI:10.1167/iovs.04-1064

Diabetic retinopathy (DR), a microvascular complication of diabetes mellitus, is one of the leading causes of adult blindness in developed countries. Despite its prevalence and severity, the molecular mechanisms underlying DR have not been fully elucidated. Various mechanisms have been proposed, such as increased flux through polyol[1] and hexosamine pathways,[2,3] nonenzymatic glycosylation, increased formation of advanced glycation end products (AGEs),[4,5] protein kinase C activation,[6] glucose-induced DNA damage,[7] and oxidative stress.[8] All these pathologic changes appear to be initiated by chronic exposure of the retinal microvasculature to increased blood glucose concentrations. Clinical studies have demonstrated a strong association between long-term glycemic control and the development and progression of diabetic retinopathy.[9–12] On a cellular level, prolonged hyperglycemia associated with diabetes mellitus is deleterious to the retinal microvasculature and results in endothelial cell and pericyte death; formation of microaneurysms and acellular capillaries; thickening of basement membranes; and, in severe cases, retinal neovascularization.[13]

Glucose is the major energy source for the retina, and its transport from the blood to the neuroretina is mediated by a facilitative, sodium-independent glucose transporter known as GLUT1.[14–16] The transport of glucose into the retina by GLUT1 exceeds its phosphorylation by hexokinase, the rate-limiting step in retinal glucose metabolism.[17,18] Consequently, measurable free glucose is available as a substrate for biochemical processes thought to be responsible for the development of DR. It is also possible, however, that the effects of elevated glucose concentrations may be mediated by the binding of AGEs to endothelial cell surface receptors (RAGE).[19] Binding of AGE to its receptors has been shown to result in activation of specific signaling pathways,[20] as well as increased oxidative stress[21] and apoptosis[22,23] in vascular cells.

The c-Jun N-terminal kinase pathway is important in modulating cellular responses to stress. Increased oxidative stress has been implicated in several animal models of diabetes through activation of the c-Jun N-terminal kinase, such as β-cell dysfunction and the formation of coronary atherosclerosis.[24,25] JNK is a stress-induced protein kinase and is involved in regulation of gene expression and stabilization through phosphorylation of Jun and other proteins.[26] Only the phosphorylated JNK (phospho-JNK), which is translocated to the nucleus, activates c-Jun.[27] The assembly of JNK and its upstream kinases (MAPKK and MAPKKK) requires molecular scaffold proteins, the JNK interacting proteins (JIPs).[28,29] Several studies have reported that JNK activity is increased in response to diabetes, and elevated JNK activity interferes with insulin action both in cell culture and in animal models.[30–33]

From the Departments of [1]Internal Medicine and [5]Physiology and the [6]JDRF Center for Complications in Diabetes, University of Michigan Medical School, Ann Arbor, Michigan; the [2]Department of Pharmaceutical Science, Toyama Medical and Pharmaceutical University, Toyama, Japan; the [3]Department of Molecular Biopharmacy and Genetics, Graduate School of Pharmaceutical Sciences, Tohoku University, Sendai, Japan; and the [4]Pennington Biomedical Research Center, Louisiana State University, Baton Rouge, Louisiana.

Supported by an ARVO/Novartis Research Fellowship Grant (JZ) and the JDRF Center for Complications in Diabetes (AKK) and in part by National Institutes of Health Grant RPO60DK-20572, which supports the Michigan Diabetes Research and Training Center.

Submitted for publication September 8, 2004; revised November 15, 2004, and March 22, 2005; accepted April 11, 2005.

Disclosure: **J. Zhou**, None; **B.K. Deo**, None; **K. Hosoya**, None; **T. Terasaki**, None; **I.G. Obrosova**, None; **F.C. Brosius, III**, None; **A.K. Kumagai**, None

The publication costs of this article were defrayed in part by page charge payment. This article must therefore be marked "*advertisement*" in accordance with 18 U.S.C. §1734 solely to indicate this fact.

Corresponding author: Arno K. Kumagai, Department of Internal Medicine, 5570 MSRB-2, Box 0678, Ann Arbor, MI 48109-0678; akumagai@umich.edu.

To understand whether increased intracellular glucose concentrations potentiate oxidative stress and activate the JNK signaling pathway in retinal endothelial cells, we established lines of stable transfected GLUT1-overexpressing rat retinal endothelial cells. In this report, we demonstrate that increased GLUT1 expression results in an increase in intracellular glucose and elevated oxidative stress and JNK phosphorylation in this cell line. These results indicate that the JNK signaling pathway is activated in response to increased glucose flux.

METHODS

Antibodies

The anti-phosphoJNK and anti-total JNK antibodies were from Santa Cruz Biotechnology, Inc. (Santa Cruz, CA); the anti-malondialdehyde (MDA) antibody from Abcam, Inc. (Cambridge, MA); and the anti-rabbit and anti-mouse antibodies coupled to horseradish peroxidase from GE Healthcare (Piscataway, NJ). Staining of transferred proteins on the Western blot membranes, as well as an anti-GAPDH monoclonal antibody (Advanced Immunochemical, Inc., Long Beach, CA) were used as internal loading controls. A polyclonal antibody raised against a purified human erythrocyte glucose transporter (GLUT1) was the kind gift of Christin Carter-Su (University of Michigan) and the polyclonal anti-JIP-1 antibodies were kindly provided by Benjamin Margolis (University of Michigan). The anti-GLUT1 and anti-JIP-1 antibodies have been characterized previously.[34,35]

Cell Culture

An immortalized rat retinal endothelial cell line TRiBRB, which was established from retinal capillaries isolated from transgenic rats carrying temperature-sensitive SV-40 large T antigen gene, was used in this study.[36] Although experiments investigating the endothelial cell biology of diabetic microvascular complications have frequently been performed in primary endothelial cell cultures of bovine or human origin, the well-known difficulty in transfecting retinal endothelial cells with exogenous DNA prevented use of a primary retinal endothelial cell culture model in these experiments.[37] The conditionally immortalized rat retinal endothelial cell line, TRiBRB, was therefore used to create stable retinal endothelial cell overexpression of GLUT1. TRiBRB cells are a well-described line that have typical characteristics of primary retinal endothelial cells in culture, including spindle-shaped morphology, expression of factor VIII, VEGF receptor-2, and p-glycoprotein, as well as uptake of acetylated LDL, and facilitated transport of glucose, oxidized vitamin C, and amino acids.[36,38–41] The cells were grown in DMEM (Invitrogen, Carlsbad, CA) supplemented with fetal bovine serum (10%), endothelial cell growth factor (15 μg/mL; Roche, Indianapolis, IN), heparin (100 μg/mL), and antibiotics and antimycotics (100 U/mL penicillin, 100 μg/mL streptomycin, and 250 ng/mL amphotericin B; Sigma-Aldrich, St. Louis, MO). To establish stable transfected cells, full-length human GLUT1 cDNA (a gift from Michael Mueckler, Washington University, St. Louis, MO) was subcloned into pcDNA3.1 at the *Bam*HI site (BD-Clontech, Palo Alto, CA) and transfected into TRiBRB cells. A pcDNA3.1 was also transfected into TRiBRB cells as a vector control. Stable transfected cells were propagated through G418 selection at 32°C. Cells were then switched to 37°C for all experiments. It has been shown that SV40 expression is substantially reduced after 1 to 2 days of culture at a nonpermissive temperature.[36] Expression of GLUT1 was determined by Western blot analysis.[42] All cells were collected at the same passages and same cell density.

Intracellular Glucose Measurement

Intracellular glucose concentration was measured by gas chromatography (GC)-mass spectrometry. Briefly, vector control and GLUT1-overexpressing cells were cultured in complete medium, as stated earlier including 5 mM glucose and allowed to grow to 90% confluence in six-well plates. Cells were then washed three times in cold 1× phosphate-buffered saline. After they were freeze-thawed three times, aliquots (200 μL) of supernatants were treated with trichloroacetic acid (final concentration 5% trichloroacetic acid [TCA]) and then derivatized with hydroxylamine and 4-dimethylamino pyridine.[43] A GC-mass spectrometer (5972 series; Hewlett Packard, Palo Alto, CA) was used to measure glucose concentrations. Aliquots were taken to determine total protein amount using bicinchoninic acid (BCA) protein assays, based on the manufacturer's instructions (Pierce Biotechnology, Inc., Rockford, IL). Intracellular glucose concentrations were compared between GLUT1-overexpressing and vector control cells.

Intracellular Reactive Oxygen Species Measurement

The intracellular reactive oxygen species was determined by a fluorescence detection method based on the oxidation of 5- (and -6)-chloromethyl-2′,7′- dichlorodihydrofluorescein diacetate, acetyl ester (CM-H_2DCFDA; Molecular Probes Inc., Eugene, OR).[8] GLUT1-overexpressing and vector control cells were grown in complete medium, as stated in the prior section, including 5 mM glucose, and allowed to grow in six-well plates until 90% confluence was achieved. CM-H_2DCFDA was added for 1 hour (20 μM) and fluorescence was analyzed by a cell sorter (Elite ESP; Beckman Coulter, Hialeah, FL) using excitation and emission wavelengths of 495 and 525 nm, respectively.

RNA Extraction, cDNA Microarray, and Northern Blot Analyses

GLUT1-overexpressing and vector control cells were grown in 5 mM glucose for 5 days to 90% confluence. Vector control and GLUT1-overexpressing cells were homogenized in extraction reagent (TRIzol; Invitrogen, Carlsbad, CA). Total RNA was extracted and further purified using an RNA cleanup procedure (RNeasy; Qiagen, Valencia, CA). RNA yields were assessed by absorbance at 260 nm, and the quality was confirmed on agarose-formaldehyde gels.

The cDNA microarray analysis was performed in conjunction with the Michigan NIDDK Biotechnology Core using a rat genome microarray (U34 chips; Affymetrix, Inc., Santa Clara, CA) containing gene expression data for >8000 known genes. Total RNA was extracted and purified as just described. Comparisons were made between GLUT1-overexpressing and vector control cells at normal glucose concentrations, to determine whether GLUT1 overexpression per se causes changes in gene expression profiles. Gene expression patterns detected by cDNA microarray analysis were confirmed in replicated experiments. Changes in gene expression that met a minimum of a twofold change, compared with control samples, were confirmed by Northern blot analysis.

To perform Northern blot analysis, total RNA was fractionated on agarose-formaldehyde gel electrophoresis. RNAs were transferred to membranes (Nytran SuPerCharge membrane; Schleicher & Schuell, Keene, NH) and hybridized with rat JIP-1b cDNA fragment and a housekeeping gene acidic ribosomal phosphoprotein PO (ARP/36B4) cDNA probe labeled with [α-^{32}P]dCTP by random primer labeling (GE Healthcare). The intensity of each band was visualized and quantified (PhosphorImager and Quantity One software; Bio-Rad, Hercules, CA).

Immunoblot and Immunoprecipitation

Vector control and GLUT1-overexpressing cells were washed three times in cold 1× phosphate-buffered saline and lysed in lysis buffer (1% SDS, 62.5 μM Tris [pH 6.8], 10% glycerol). As positive controls in MDA detection, both vector and GLUT1-overexpressing cells were treated with 80 μM H_2O_2 for 1 hour at 37°C. Cells were then rinsed twice with PBS. Proteins were resolved by electrophoresis on 10% SDS polyacrylamide gels, transferred to membranes (Hybond-P; GE Healthcare), and immuno-

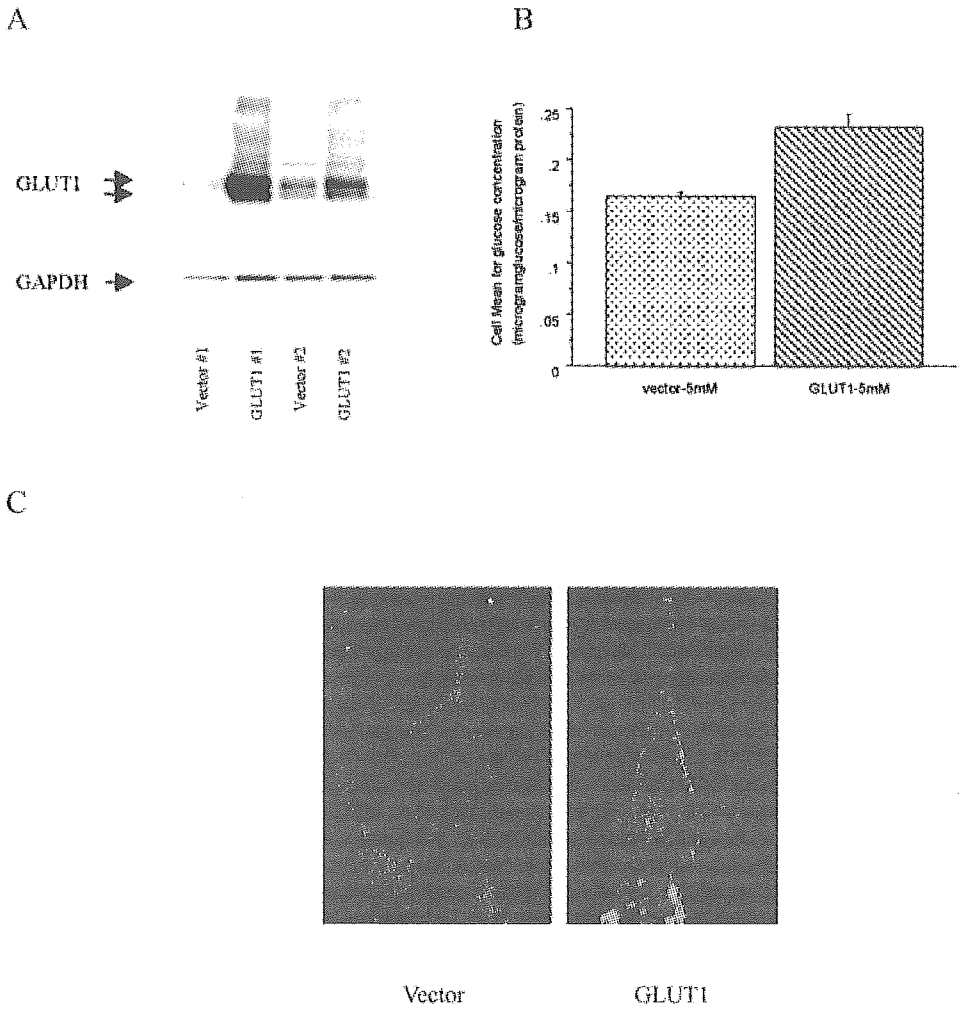

FIGURE 1. Vector control and GLUT-overexpressing cells[b]. (**A**) Western blot analysis for GLUT1 in vector and GLUT-overexpressing cells from two independent sets of clones (clone 1 and clone 2). Each lane contains 10 μg protein from whole-cell lysate. The membrane was first probed with anti-GLUT1 antibody, and then it was stripped and reprobed with anti-GAPDH antibody to serve as an internal loading control. (**B**) Intracellular glucose measurements in vector and GLUT1-overexpressing cells, by GC-mass spectrometry. Cells were cultured in medium containing 5 mM glucose. Data are the mean ± SE ($n = 6$). There was a statistically significant difference between the vector and GLUT1-overexpressing cells ($P = 0.0003$, Student's t-test). (**C**) Immunocytochemistry for GLUT1 in vector control and GLUT1-overexpressing cells. GLUT1 expression was detected by confocal microscopy. Magnification, ×600.

blotted with antibodies against GLUT1, total JNK, phosphoJNK, and MDA, followed by secondary horseradish peroxidase-anti-rabbit antibodies according to methods described previously.[42] Blots were visualized by a chemiluminescence assay (ECL-Plus; GE Healthcare, Piscataway, NJ). To verify equal loading of proteins, Western blots were stained with ponceau-S after transfer. In addition, after immunoblot, each blot was stripped and reprobed with an anti-GAPDH antibody, as an internal control.

To perform immunoprecipitation, vector control and GLUT1-overexpressing cells were washed in 1× phosphate-buffered saline and scraped with a cell scraper in lysis buffer (50 mM HEPES [pH 7.5], 10% glycerol, 150 mM NaCl, 1% Triton X-100, 1.5 mM $MgCl_2$,1 mM EGTA, 1 mM phenylmethylsulfonyl fluoride, 100 mM NaF, 200 mM sodium orthovanadate, 10 mM tetrasodium pyrophosphate, 10 mg aprotinin/mL and 10 mg leupeptin/mL).[35] Lysates (4.5 mg) were incubated with a anti-JIP-1 antibody (antiserum no. 152) and protein A agarose (RepliGen Corp., Waltham, MA) overnight at 4°C. Pellets were washed three times in washing buffer (20 mM HEPES [pH 7.5], 150 mM NaCl, 10% glycerol, and 0.1% Triton X-100) and boiled in 1× sample buffer. Supernatants were resolved by 8% SDS polyacrylamide gel electrophoresis, transferred to a membrane (Hybond-P; GE Healthcare), and immunoblotted with antibodies against JIP-1, GLUT1, total JNK, and phosphoJNK. Blots were visualized by chemiluminescence as above (ECL Plus; GE Healthcare).

Immunohistochemistry

Vector control and GLUT1-overexpressing cells were grown on chamber slides to 90% confluence. Cells were fixed with 4% paraformaldehyde for 30 minutes at room temperature and permeabilized with 0.1% Triton X-100 in 1× phosphate-buffered saline for 10 minutes. The slides were blocked with 1% goat serum for 1 hour and incubated with either anti-GLUT1 (1:500 dilution) or anti-JIP-1 (1:250 dilution) overnight. After washing, the slides were incubated with goat anti-rabbit-FITC (1:200 dilution; Molecular Probes) for 1 hour, and mounted (Prolong; Molecular Probes) and viewed with a laser scanning confocal microscope (model OZ; Noran Instruments, Middleton, WI).

Statistical Analysis

Comparisons between vector control and GLUT1-overexpressing cells were made with Student's t-test. $P < 0.05$ was considered significant.

RESULTS

Increased Glucose Flux in GLUT1-Overexpressing Cells

Under normal culture conditions, immortalized rat retinal endothelial cells overexpressing GLUT1 showed an approximate four- to eightfold increase in GLUT1 expression compared with vector control cells (Fig. 1A). Such levels of expression were confirmed by Western blot in every experiment performed. Increased GLUT1 expression resulted in increased intracellular glucose, as determined by GC-mass spectrometry (Fig. 1B). There was an average 40% increase in intracellular glucose in GLUT1-overexpressing cells compared with vector control

cells, and the increase was statistically significant ($P = 0.0003$; Fig. 1B). Immunohistochemistry confirmed membrane expression of GLUT1 protein in both vector control and GLUT1-overexpressing cells (Fig 1C). Increased GLUT1 expression was also visible in GLUT1-overexpressing cells, with much of GLUT1 protein localized in the cytoplasmic membrane.

Increased Oxidative Stress in GLUT1-Overexpressing Cells

The presence of free glucose in the retinal endothelial cells may provide a substrate for a variety of biochemical processes. We examined the possibility that GLUT1-overexpression induces oxidative stress in TRiBRB cells. GLUT1-overexpressing and vector control cells were incubated with CM-H_2DCFDA (20 μM) for 1 hour, and the fluorescence was measured by flow cytometry (FACScan; BD Biosciences, Franklin Lakes, NJ). As shown in Figure 2A, there was approximately an 80% increase in generation of DCF-sensitive ROS in GLUT1-overexpressing compared with vector control cells, a statistically significant increase ($P < 0.0001$). To determine whether lipid peroxidation products were increased with GLUT1-overexpression, GLUT1-overexpressing and vector control cells were grown in 5 mM glucose, and Western blot analysis was performed using antibody against MDA-protein addicts. Identical cultures were treated with 80 μM H_2O_2 for 1 hour as positive controls. As shown in Figure 2B, there was increased lipid peroxidation in GLUT1-overexpressing cells as determined by increased MDA-modified protein addicts in Western blot analysis (Fig. 2B). The most prominent MDA-modified protein adducts were of higher molecular weight, approximately 200 and 80 kDa, in GLUT1-overexpressing cells compared to vector control cells.

Increased JNK Phosphorylation in GLUT1-Overexpressing Cells

Increased JNK activity in response to high glucose has been reported in human umbilical vein endothelial cells.[44] To assess whether increased glucose flux through increased GLUT1 expression also results in the phosphorylation of JNK in retinal endothelial cells, we performed Western blot analysis and probed the blots with anti-phosphoJNK and total JNK. As shown in Figure 3, there was a basal level of JNK phosphorylation in vector control cells. Increased GLUT1 expression and increased glucose flux resulted in an increase in JNK phosphorylation. There was no detectable change in total JNK (Fig. 3). Western blot with an anti-p38 antibody revealed no change in p38 protein expression (data not shown).

Increased JIP-1 Expression in GLUT1-Overexpressing Cells

To identify additional molecular changes in GLUT1-overexpressing cells, cDNA microarray analysis was performed using a rat genome microarray (Set U34; Affymetrix, Inc.). We found increased JIP-1 gene expression among the upregulated genes. JIP-1 expression was increased more than twofold in two replicates (Fig. 4A). To confirm the observed changes in JIP-1 expression, we performed Northern blot analysis. As shown in Figure 4B, there was an approximate 80% increase in JIP-1 expression in GLUT1-overexpressing cells compared with that in vector control cells. The expression of transcripts of enzymes involved in glycolytic, polyol, and hexosamine pathways were unchanged in the overexpressing cells compared with the vector control (data not shown).

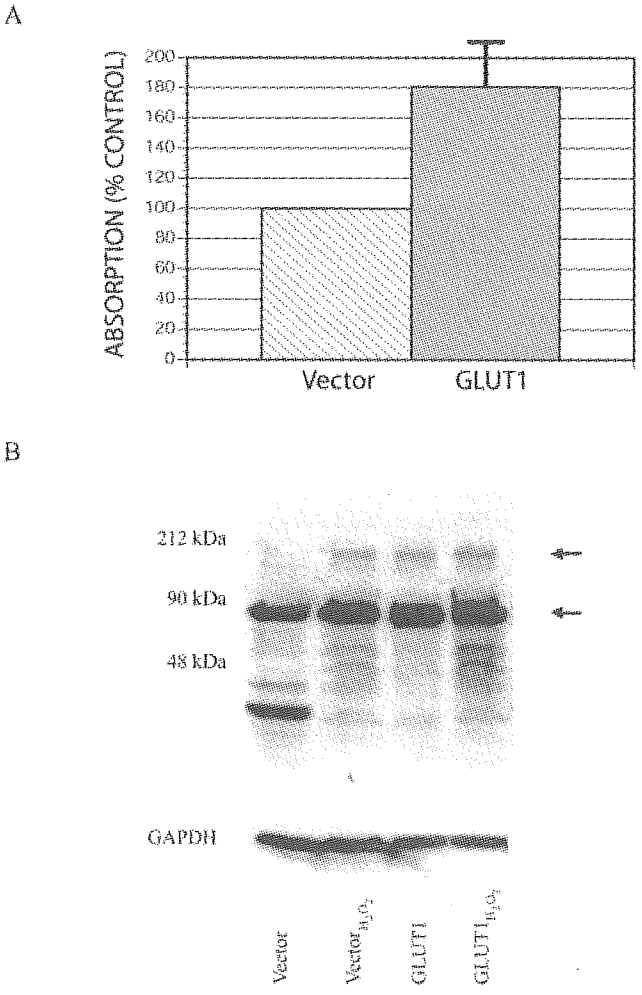

FIGURE 2. Oxidative stress measurements in vector and GLUT1-overexpressing cells. (**A**) DCF measurement in vector and GLUT1-overexpressing cells. Cells were grown in complete medium containing 5 mM glucose and allowed to grow in six-well plates until 90% confluence was achieved. CM-H_2DCFDA was added for 1 hour (20 μM) and analyzed by flow cytometry, using excitation and emission wavelengths of 495 and 525 nm, respectively. (**B**) Western blot for MDA-modified protein adducts in vector and GLUT1-overexpressing cells. Each lane contains 30 μg protein from whole-cell lysate. Vector control and GLUT1-overexpressing cells treated with 80 μM H_2O_2 were used as a positive control for detecting MDA-modified protein adducts. After probing with anti-MDA antibody, the membrane was stripped and reprobed with GAPDH as the loading control.

Association of JIP-1 with PhosphoJNK

Endogenous JIP-1 protein has been detected mainly in pancreatic islet and neuronal cells.[35,45] To determine whether JIP-1 protein is expressed in retinal endothelial cells, we performed immunoprecipitation using whole-cell lysates (4.5 mg).[35] In both vector control and GLUT1-overexpressing cells, a prominent band corresponding to 90 kDa was detected by antibodies against both JIP-1 carboxyl-terminal peptide (antiserum no. 176) and GST-JIP-1 Src homology 3 domain fusion protein (antiserum no. 152),[35] which was consistent with JIP-1 detected in neuronal cells (Fig. 5A).[35,45] As a JNK scaffold protein, JIP-1 binds to three kinases, MLK3, MAP2K7, and JNK, to form a signaling complex.[28,46] In both vector control and GLUT1-overexpressing cells, phosphorylated JNK was found to coimmunoprecipitate with JIP-1 (Fig. 5B), which is consistent

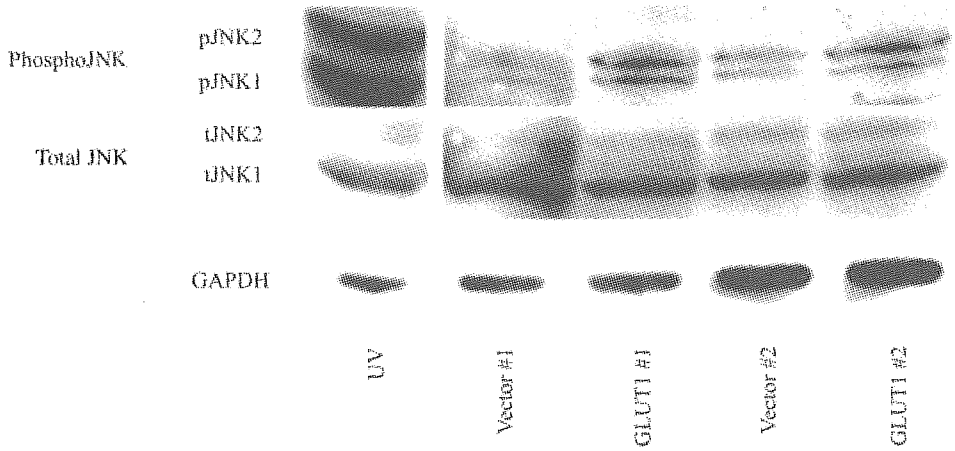

FIGURE 3. Western blot of phosphorylated JNK and total JNK in vector control and GLUT1-overexpressing cells. Vector control and GLUT1-overexpressing cells from two independent clone sets were cultured in medium containing 5 mM glucose. Each lane contains 20 μg protein from whole-cell lysate, except for the UV control lane (5 μg/lane). Human embryonic kidney 293 cells were treated with 400 μJ of UV light to induce JNK phosphorylation and served as positive control for phosphorylated JNK. The membrane was first probed with anti-phosphorylated JNK. The membrane was then stripped and reprobed with anti-total JNK antibody. After the second stripping, the membrane was probed with anti-GAPDH antibody, as an internal loading control.

A

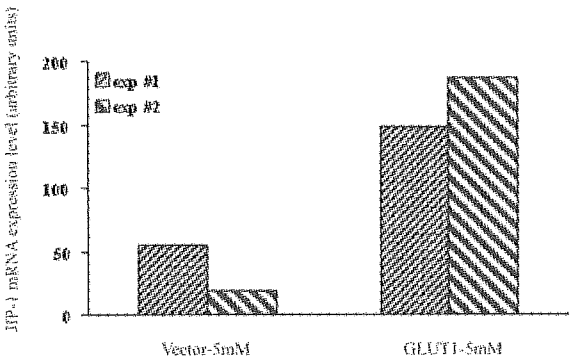

B

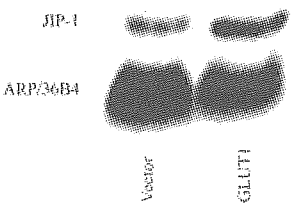

FIGURE 4. Upregulation of the JIP-1 gene in GLUT1-overexpressing cells compared with vector control cells, detected by cDNA microarray analysis (**A**). GLUT1-overexpressing and vector control cells were cultured in medium containing 5 mM glucose for 5 days. Results are from two independent cDNA microarray analyses. JIP-1 was upregulated by more than twofold in both experiments. (**B**) Northern blot of JIP-1 in vector control and GLUT1-overexpressing cells. Total RNA was extracted from vector control and GLUT1-overexpressing cells. Each lane contained 25 μg total RNA. The membrane was probed with a ^{32}P-labeled JIP-1 fragment and ARP/36B4.

with the role of JIP-1 as a scaffold protein essential in JNK activation. Immunoprecipitation also showed a basal level of JNK phosphorylation associated with JIP-1 in vector control cells. JIP-1 has been reported to be in direct contact with cell surface receptors, guanine exchange factor, and motor kinesin,[35,47–49] however, GLUT1 did not coimmunoprecipitate with JIP-1 (data not shown).

Subcellular Localization of JIP-1 in Retinal Endothelial Cells

To determine the localization of endogenous JIP-1 in retinal endothelial cells, both vector control and GLUT1-overexpressing cells were stained by indirect immunofluorescence. JIP-1 was found to be predominantly localized in the cytoplasm, especially in the perinuclear area. Confocal microscopy revealed that a small amount of JIP-1 was localized in the nucleus (Fig. 6). The pattern of JIP-1 staining was similar in both vector control and GLUT1-overexpressing cells.

Discussion

In this study, we report changes in oxidative stress and JNK phosphorylation in stable transfected GLUT1-overexpressing rat retinal endothelial cells in response to increased intracellular glucose. Our results demonstrate that increased oxidative stress and JNK phosphorylation resulted from increased glucose flux through increased GLUT1 expression. The increased JNK phosphorylation probably occurs through upregulation of JIP-1, as evidenced by physical association of JIP-1 with phosphorylated JNK protein.

Increased glucose has been shown to generate increased reactive oxygen species (ROS) in cell types susceptible to hyperglycemic damage, such as endothelial cells and mesangial cells.[50,51] In our study, we found an approximate 80% increase in generation of cytosolic ROS, which was detected by DCF in GLUT1-overexpressing compared with vector control cells. It has been suggested that high-glucose–induced ROS production mainly consists of hydrogen peroxide.[51] In mesangial cells, H_2O_2 was produced through increased glucose uptake and glucose metabolism rather than glucose auto-oxidation and can

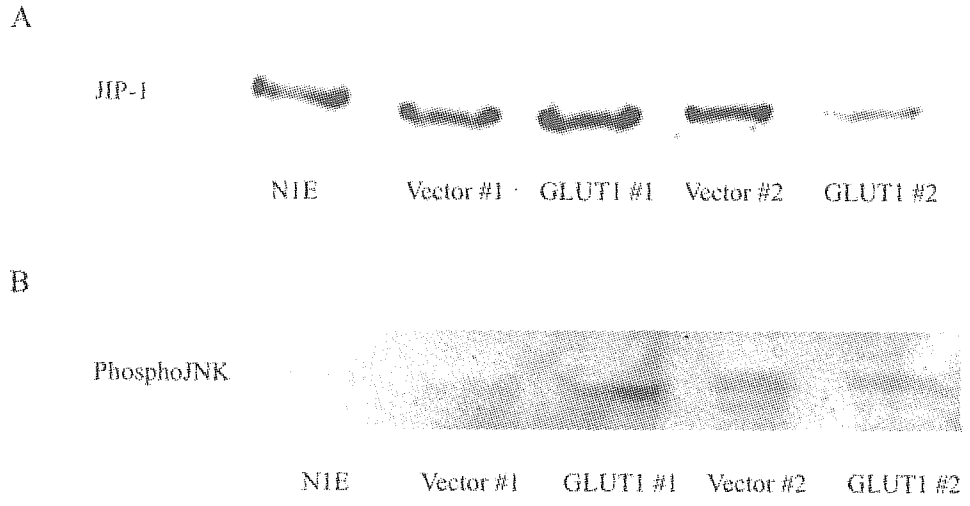

FIGURE 5. Coimmunoprecipitation of JIP-1 and phosphorylated JNK in both vector and GLUT1-overexpressing cells. (**A**) Lysates from vector and GLUT1-overexpressing cells were immunoprecipitated with anti-JIP-1 antibody (antiserum no. 152) and immunoblotted with anti-JIP-1 (antiserum no. 176). Mouse neuroblastoma N1E-115 cells were used as a positive control for JIP-1. Two sets of independent clones were used in the experiments (marked #1 and #2). (**B**) After probing with anti-JIP-1 antibody (antiserum no. 176), the membrane was stripped and reprobed with anti-phosphorylated JNK antibody to detect the presence of phosphorylated JNK.

be effectively inhibited by catalase.[51] Although the ROS species generated in retinal endothelial cells remains to be determined, our initial experiments did not find significant changes in catalase activity. Our study also detected increased MDA-modified protein addicts at higher molecular weight (approximately 80 and 200 kDa), which suggested increased lipid peroxidation—a marker of oxidative stress-in GLUT1-overexpressing cells. Previous studies in diabetic subjects have shown that lipid peroxidation in both plasma and the vitreous body is linked to the development and progression of diabetic retinopathy. The reduction of lipid peroxidation in patients with rigorously controlled diabetes conferred a 50% lower risk of development of proliferative retinal changes, compared with standard glucose control subjects.[52]

Recent studies found that the JNK pathway plays an important role in the development and progression of diabetes and its complications.[30–33,44,53–55] Increased ambient glucose results in growth retardation in several primary endothelial cell cultures, such as human umbilical vein endothelial cells (HUVECs), bovine pulmonary artery endothelial cells (PAECs), and cultured human endothelial cells.[56–58] The inhibition of cell growth has been suggested to be associated with JNK activation.[53] JNK activation induced by increased glucose was detected both in neurons and endothelial cells.[53,54] Our data also showed increased JNK phosphorylation to be associated with increased glucose flux and GLUT1 overexpression in rat retinal endothelial cells.

The identification of JIP-1 upregulation and increased JNK phosphorylation in the present study suggests that JIP-1 potentiates JNK activation in response to increased glucose flux through GLUT1 overexpression. This raises intriguing questions regarding the molecular events that connect increased glucose flux and increased JNK activity. JIP-1/IB1 has been reported as a nuclear protein that binds to the GLUT2 promoter and regulates GLUT2 expression in islet cells.[45] In neurons, JIP-1 is located in cytoplasm. On neuronal differentiation, JIP-1 concentrates at the extending end of neurites.[35] In our study, JIP-1 was mainly localized in the cytoplasm, especially the perinuclear area. JIP-1 has been shown to interact with several membrane receptors to form a signaling complex.[47,48,59] JIP-1 has also been detected to interact with an exchange factor for the small GTPase RhoA and molecular motor kinesin to regulate cytoskeleton rearrangement in neuronal cells.[35,49] Our study did not find a physical association between JIP-1 and GLUT1.

Increased oxidative stress has been linked to the activation of JNK pathway in many cell types.[60,61] Hydrogen peroxide produced during oxidative stress has been shown to be a potent activator that induces JNK activation in skeletal muscle fibers.[60] Studies in bovine lung microvascular endothelial cells have indicated that increased glutathione reductase activity inhibits JNK activation.[61] Although we did not determine whether increased lipid peroxidation is directly linked to increased JNK phosphorylation in the present study, given the above experimental observations conducted in other cell types, we speculate that there is a mechanistic link between increased lipid peroxidation and JNK phosphorylation in response to increased glucose flux through increased GLUT1 expression in rat retinal endothelial cells. The pathologic consequences associated with increased oxidative stress and JNK

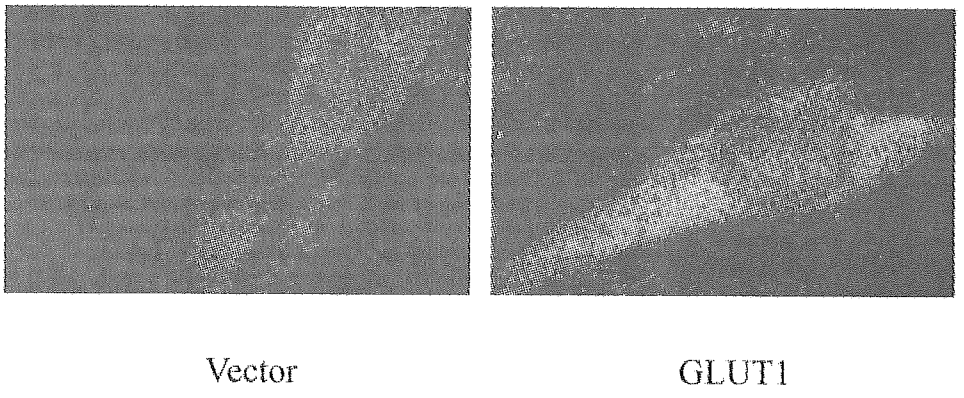

FIGURE 6. Immunocytochemistry for JIP-1 in vector control and GLUT1-overexpressing cells grown on chambered slides. JIP-1 protein was detected with anti-JIP-1 antibody (antiserum no. 152). JIP-1 expression was visualized by confocal microscopy. Magnification, ×600.

phosphorylation in retinal endothelial cells remain to be determined.

Acknowledgments

The authors thank Kelli Sullivan, Stephen Lentz, and the staff of the JDRF Morphology Core for assistance with morphologic analysis and Martin J. Stevens and Judy Grossi for help with the GC-Mass spectrometry measurements.

References

1. Robison WG, Kinoshita JH, Kador PF. The polyol pathway in retinal microangiopathy. *Drugs*. 1986;32:19-22.
2. Heath H, Paterson RA, Hart JC. Changes in the hydroxyproline, hexosamine and sialic acid of the diabetic human and beta, beta'-iminodipropionitrile-treated rat retinal vascular systems. *Diabetologia*. 1967;3:515-518.
3. Nakamura M, Barber AJ, Antonetti DA, et al. Excessive hexosamines block the neuroprotective effect of insulin and induce apoptosis in retinal neurons. *J Biol Chem*. 2001;276:43748-43755.
4. Stitt AW, Jenkins AJ, Cooper ME. Advanced glycation end products and diabetic complications. *Expert Opin Investig Drugs*. 2002;11:1205-1223.
5. Stitt AW, Li YM, Gardiner TA, Bucala R, Archer DB, Vlassara H. Advanced glycation end products (AGEs) co-localize with AGE receptors in the retinal vasculature of diabetic and of AGE-infused rats. *Am J Pathol*. 1997;150:523-531.
6. King GL, Kunisaki M, Nishio Y, Inoguchi T, Shiba T, Xia P. Biochemical and molecular mechanisms in the development of diabetic vascular complications. *Diabetes*. 1996;45:S105-S108.
7. Lorenzi M, Montisano DF, Toledo S, Barrieux A. High glucose induces DNA damage in cultured human endothelial cells. *J Clin Invest*. 1986;77:322-325.
8. Nishikawa T, Edelstein D, Du XL, et al. Normalizing mitochondrial superoxide production blocks three pathways of hyperglycaemic damage. *Nature*. 2000;404:787-790.
9. Klein R, Klein BE, Moss SE, Davis MD, DeMets DL. The Wisconsin epidemiologic study of diabetic retinopathy. III. Prevalence and risk of diabetic retinopathy when age at diagnosis is 30 or more years. *Arch Ophthalmol*. 1984;102:527-532.
10. Klein R, Klein BE, Moss SE, Davis MD, DeMets DL. The Wisconsin epidemiologic study of diabetic retinopathy. II. Prevalence and risk of diabetic retinopathy when age at diagnosis is less than 30 years. *Arch Ophthalmol*. 1984;102:520-526.
11. The Diabetes Control, Complications Trial Research Group. The effect of intensive treatment of diabetes on the development and progression of long-term complications in insulin-dependent diabetes mellitus. *N Engl J Med*. 1993;329:977-986.
12. UKPDS. Intensive blood-glucose control with sulphonylureas or insulin compared with conventional treatment and risk of complications in patients with type 2 diabetes (UKPDS 33). UK Prospective Diabetes Study (UKPDS) Group. *Lancet*. 1998;352:837-853.
13. Cogan D, Toussaint D, Kuwabara T. Retinal vascular patterns. IV. Diabetic retinopathy. *Arch Ophthalmol*. 1961;66:366-378.
14. Kumagai AK, Glasgow BJ, Pardridge WM. GLUT1 glucose transporter expression in the diabetic and nondiabetic human eye. *Invest Ophthalmol Vis Sci*. 1994;35:2887-2894.
15. Harik SI, Kalaria RN, Whitney PM, et al. Glucose transporters are abundant in cells with "occluding" junctions at the blood-eye barriers. *Proc Natl Acad Sci U S A*. 1990;87:4261-4264.
16. Takata K, Hirano H, Kasahara M. Transport of glucose across the blood-tissue barriers. *Int Rev Cytol*. 1997;172:1-53.
17. Berkowitz BA, Garner MH, Wilson CA, Corbett RJ. Nondestructive measurement of retinal glucose transport and consumption in vivo using NMR spectroscopy. *J Neurochem*. 1995;64:2325-2331.
18. Olgemoller B, Schleicher ED, Gerbitz KD. Differential kinetics of glucose metabolism in porcine retinal and aortic endothelial cells. *J Clin Chem Clin Biochem*. 1990;28:15-17.
19. Schmidt AM, Hori O, Cao R, et al. RAGE: a novel cellular receptor for advanced glycation end products. *Diabetes*. 1996;45:S77-S80.
20. Lander HM, Tauras JM, Ogiste JS, Hori O, Moss RA, Schmidt AM. Activation of the receptor for advanced glycation end products triggers a p21(ras)-dependent mitogen-activated protein kinase pathway regulated by oxidant stress. *J Biol Chem*. 1997;272:17810-17814.
21. Yan SD, Schmidt AM, Anderson GM, et al. Enhanced cellular oxidant stress by the interaction of advanced glycation end products with their receptors/binding proteins. *J Biol Chem*. 1994;269:9889-9897.
22. Min C, Kang E, Yu SH, Shinn SH, Kim YS. Advanced glycation end products induce apoptosis and procoagulant activity in cultured human umbilical vein endothelial cells. *Diabetes Res Clin Pract*. 1999;46:197-202.
23. Yamagishi S, Inagaki Y, Okamoto T, et al. Advanced glycation end product-induced apoptosis and overexpression of vascular endothelial growth factor and monocyte chemoattractant protein-1 in human-cultured mesangial cells. *J Biol Chem*. 2002;277:20309-20315.
24. Kawamori D, Kajimoto Y, Kaneto H, et al. Oxidative stress induces nucleo-cytoplasmic translocation of pancreatic transcription factor PDX-1 through activation of c-Jun NH(2)-terminal kinase. *Diabetes*. 2003;52:2896-2904.
25. Zhang L, Zalewski A, Liu Y, et al. Diabetes-induced oxidative stress and low-grade inflammation in porcine coronary arteries. *Circulation*. 2003;108:472-478.
26. Kallunki T, Deng T, Hibi M, Karin M. c-Jun can recruit JNK to phosphorylate dimerization partners via specific docking interactions. *Cell*. 1996;87:929-939.
27. Gupta S, Campbell D, Derijard B, Davis RJ. Transcription factor ATF2 regulation by the JNK signal transduction pathway. *Science*. 1995;267:389-393.
28. Whitmarsh AJ, Cavanagh J, Tournier C, Yasuda J, Davis RJ. A mammalian scaffold complex that selectively mediates MAP kinase activation. *Science*. 1998;281:1671-1674.
29. Dickens M, Rogers JS, Cavanagh J, et al. A cytoplasmic inhibitor of the JNK signal transduction pathway. *Science*. 1997;277:693-696.
30. Carlson CJ, Koterski S, Sciotti RJ, Poccard GB, Rondinone CM. Enhanced basal activation of mitogen-activated protein kinases in adipocytes from type 2 diabetes: potential role of p38 in the downregulation of GLUT4 expression. *Diabetes*. 2003;52:634-641.
31. Hirosumi J, Tuncman G, Chang L, et al. A central role for JNK in obesity and insulin resistance. *Nature*. 2002;420:333-336.
32. Fujishiro M, Gotoh Y, Katagiri H, et al. Three mitogen-activated protein kinases inhibit insulin signaling by different mechanisms in 3T3-L1 adipocytes. *Mol Endocrinol*. 2003;17:487-497.
33. Fernyhough P, Gallagher A, Averill SA, et al. Aberrant neurofilament phosphorylation in sensory neurons of rats with diabetic neuropathy. *Diabetes*. 1999;48:881-889.
34. Tai PK, Liao JF, Chen EH, Dietz J, Schwartz J, Carter-Su C. Differential regulation of two glucose transporters by chronic growth hormone treatment of cultured 3T3-F442A adipose cells. *J Biol Chem*. 1990;265:21828-21834.
35. Meyer D, Liu A, Margolis B. Interaction of c-Jun amino-terminal kinase interacting protein-1 with p190 rhoGEF and its localization in differentiated neurons. *J Biol Chem*. 1999;274:35113-35118.
36. Hosoya K, Tomi M, Ohtsuki S, et al. Conditionally immortalized retinal capillary endothelial cell lines (TR-iBRB) expressing differentiated endothelial cell functions derived from a transgenic rat. *Exp Eye Res*. 2001;72:163-172.
37. Tanner FC, Carr DP, Nabel GJ, Nabel EG. Transfection of human endothelial cells. *Cardiovasc Res*. 1997;35:522-528.
38. Tomi M, Hosoya K, Takanaga H, Ohtsuki S, Terasaki T. Induction of xCT gene expression and L-cystine transport activity by diethyl maleate at the inner blood-retinal barrier. *Invest Ophthalmol Vis Sci*. 2002;43:774-779.
39. Hosoya K, Kondo T, Tomi M, Takanaga H, Ohtsuki S, Terasaki T. MCT1-mediated transport of L-lactic acid at the inner blood-retinal barrier: a possible for delivery of monocarboxylic acid drugs to the retina. *Pharm Res*. 2001;18:1669-1676.

40. Hosoya K, Minamizono A, Katayama K, Terasaki T, Tomi M. Vitamin C transport in oxidized form across the rat blood-retinal barrier. *Invest Ophthalmol Vis Sci.* 2004;45:1232-1239.
41. Hosoya K, Saeki S, Terasaki T. Activation of carrier-mediated transport of L-cystine at the blood-brain and blood-retinal barriers in vivo. *Microvasc Res.* 2001;62:136-142.
42. Sone H, Deo BK, Kumagai AK. Enhancement of glucose transport by vascular endothelial growth factor in retinal endothelial cells. *Invest Ophthalmol Vis Sci.* 2000;41:1876-1884.
43. Guerrant G, Moss C. Determination of monosaccharides as aldononitrile, O-methyloxime, alditol, and cyclitol acetate derivatives by gas chromatography. *Anal Chem.* 1984;56:633-638.
44. Ho FM, Liu SH, Liau CS, Huang PJ, Lin-Shiau SY. High glucose-induced apoptosis in human endothelial cells is mediated by sequential activations of c-Jun NH(2)-terminal kinase and caspase-3. *Circulation.* 2000;101:2618-2624.
45. Bonny C, Nicod P, Waeber G. IB1, a JIP-1-related nuclear protein present in insulin-secreting cells. *J Biol Chem.* 1998;273:1843-1846.
46. Yasuda J, Whitmarsh AJ, Cavanagh J, Sharma M, Davis RJ. The JIP group of mitogen-activated protein kinase scaffold proteins. *Mol Cell Biol.* 1999;19:7245-7254.
47. Matsuda S, Yasukawa T, Homma Y, et al. c-Jun N-terminal kinase (JNK)-interacting protein-1b/islet-brain-1 scaffolds Alzheimer's amyloid precursor protein with JNK. *J Neurosci.* 2001;21:6597-6607.
48. Gotthardt M, Trommsdorff M, Nevitt MF, et al. Interactions of the low density lipoprotein receptor gene family with cytosolic adaptor and scaffold proteins suggest diverse biological functions in cellular communication and signal transduction. *J Biol Chem.* 2000;275:25616-25624.
49. Verhey KJ, Meyer D, Deehan R, et al. Cargo of kinesin identified as JIP scaffolding proteins and associated signaling molecules [comment]. *J Cell Biol.* 2001;152:959-970.
50. Pieper GM, Langenstroer P, Siebeneich W. Diabetic-induced endothelial dysfunction in rat aorta: role of hydroxyl radicals. *Cardiovasc Res.* 1997;34:145-156.
51. Ha H, Lee HB. Reactive oxygen species as glucose signaling molecules in mesangial cells cultured under high glucose. *Kidney Int Suppl.* 2000;77:S19-S25.
52. Augustin AJ, Dick HB, Koch F, Schmidt-Erfurth U. Correlation of blood-glucose control with oxidative metabolites in plasma and vitreous body of diabetic patients. *Eur J Ophthalmol.* 2002;12:94-101.
53. Liu W, Schoenkerman A, Lowe WL Jr. Activation of members of the mitogen-activated protein kinase family by glucose in endothelial cells. *Am J Physiol.* 2000;279:E782-E790.
54. Purves T, Middlemas A, Agthong S, et al. A role for mitogen-activated protein kinases in the etiology of diabetic neuropathy. *FASEB J.* 2001;15:2508-2514.
55. Waeber G, Delplanque J, Bonny C, et al. The gene MAPK8IP1, encoding islet-brain-1, is a candidate for type 2 diabetes. *Nat Genet.* 2000;24:291-295.
56. Curcio F, Ceriello A. Decreased cultured endothelial cell proliferation in high glucose medium is reversed by antioxidants: new insights on the pathophysiological mechanisms of diabetic vascular complications. *In Vitro Cell Dev Biol.* 1992;28A:787-790.
57. Morishita R, Aoki M, Nakamura S, et al. Potential role of a novel vascular modulator, hepatocyte growth factor (HGF), in cardiovascular disease: characterization and regulation of local HGF system. *J Atheroscler Thromb.* 1997;4:12-19.
58. Lorenzi M, Nordberg JA, Toledo S. High glucose prolongs cell-cycle traversal of cultured human endothelial cells. *Diabetes.* 1987;36:1261-1267.
59. Stockinger W, Brandes C, Fasching D, et al. The reelin receptor ApoER2 recruits JNK-interacting proteins-1 and -2. *J Biol Chem.* 2000;275:25625-25632.
60. Filosto M, Tonin P, Vattemi G, Savio C, Rizzuto N, Tomelleri G. Transcription factors c-Jun/activator protein-1 and nuclear factor-kappa B in oxidative stress response in mitochondrial diseases. *Neuropathol Appl Neurobiol.* 2003;29:52-59.
61. Hojo Y, Saito Y, Tanimoto T, et al. Fluid shear stress attenuates hydrogen peroxide-induced c-Jun NH2-terminal kinase activation via a glutathione reductase-mediated mechanism. *Circ Res.* 2002;91:712-718.